Deep–Sea Research Part I 121 (2017) 14–29

Contents lists available at ScienceDirect

Deep–Sea Research I

journal homepage: www.elsevier.com/locate/dsri

Planktonic food web structure at a coastal time-series site: I. Partitioning of microbial abundances and carbon biomass

David A. Caron[a,*], Paige E. Connell[a], Rebecca A. Schaffner[b], Astrid Schnetzer[c], Jed A. Fuhrman[a], Peter D. Countway[d], Diane Y. Kim[a]

[a] Department of Biological Sciences, University of Southern California, 3616 Trousdale Parkway, Los Angeles, CA 90089-0371, USA
[b] Maine Department of Environmental Protection, 17 State House Station, Augusta, ME 04333-0017, USA
[c] Department of Marine, Earth and Atmospheric Sciences, North Carolina State University, Raleigh, NC 27695, USA
[d] Bigelow Laboratory for Ocean Sciences, East Boothbay, ME 04544, USA

ARTICLE INFO

Keywords:
Microbial abundance
Microbial biomass
Viruses
Bacteria
Protists
Zooplankton
Time-series

ABSTRACT

Biogeochemistry in marine plankton communities is strongly influenced by the activities of microbial species. Understanding the composition and dynamics of these assemblages is essential for modeling emergent community-level processes, yet few studies have examined all of the biological assemblages present in the plankton, and benchmark data of this sort from time-series studies are rare. Abundance and biomass of the entire microbial assemblage and mesozooplankton (> 200 μm) were determined vertically, monthly and seasonally over a 3-year period at a coastal time-series station in the San Pedro Basin off the southwestern coast of the USA. All compartments of the planktonic community were enumerated (viruses in the femtoplankton size range [0.02–0.2 μm], bacteria + archaea and cyanobacteria in the picoplankton size range [0.2–2.0 μm], phototrophic and heterotrophic protists in the nanoplanktonic [2–20 μm] and microplanktonic [20–200 μm] size ranges, and mesozooplankton [> 200 μm]. Carbon biomass of each category was estimated using standard conversion factors. Plankton abundances varied over seven orders of magnitude across all categories, and total carbon biomass averaged approximately 60 μg C l^{-1} in surface waters of the 890 m water column over the study period. Bacteria + archaea comprised the single largest component of biomass (> 1/3 of the total), with the sum of phototrophic protistan biomass making up a similar proportion. Temporal variability at this subtropical station was not dramatic. Monthly depth-specific and depth-integrated biomass varied 2-fold at the station, while seasonal variances were generally < 50%. This study provides benchmark information for investigating long-term environmental forcing on the composition and dynamics of the microbes that dominate food web structure and function at this coastal observatory.

1. Introduction

The pivotal biogeochemical roles conducted by microbes in marine plankton communities (herein defined as viruses, bacteria, archaea, phototrophic and heterotrophic microbial eukaryotes) are now firmly entrenched in oceanographic paradigm (Calbet and Landry, 2004; Calbet and Saiz, 2005; Sherr et al., 2007; Suttle, 2007; Fuhrman, 2009; Church et al., 2010; Caron et al., 2012). Microbes are responsible for most of the primary production occurring in pelagic communities, they dominate several trophic interactions near the base of the food web, conduct much of the carbon and nutrient cycling, and thereby affect the concentration and overall elemental stoichiometry of suspended particulate organic matter (Martiny et al., 2016). Yet, fundamental gaps and misconceptions persist in our understanding of the relative abundances, biomasses and activities of microbial assemblages, and their relationships to larger zooplankton. For example, controversy still exists as to whether community metabolism in major oceanic realms is net autotrophic or heterotrophic (Duarte et al., 2013; Ducklow and Doney, 2013; Williams et al., 2013).

These basic uncertainties relating to standing stocks and activities have important implications for how planktonic communities function, and how they might respond to changing water chemistry and physics that are anticipated over the next few centuries. Environmental change is expected to result in restructuring of pelagic food webs with significant implications for standing stocks of various plankton groups, their trophic relationships and emergent properties of carbon utiliza-

* Corresponding author.
E-mail addresses: dcaron@usc.edu (D.A. Caron), paigeeconn@gmail.com (P.E. Connell), Becky.Schaffner@maine.gov (R.A. Schaffner), aschnet@ncsu.edu (A. Schnetzer), fuhrman@usc.edu (J.A. Fuhrman), pcountway@bigelow.org (P.D. Countway), dianekim@usc.edu (D.Y. Kim).

http://dx.doi.org/10.1016/j.dsr.2016.12.013
Received 29 April 2016; Received in revised form 11 December 2016; Accepted 20 December 2016
Available online 03 January 2017
0967-0637/

tion and energy flow (Samuelsson et al., 2002; McMahon et al., 2015). However, our limited knowledge of the details of microbial community structure constrains our ability to develop models that accurately predict ecosystem response. As a consequence, Hood et al. (2006) noted that ecosystem models of increasing complexity have often led to less, not more, predictive understanding of biological processes if the plankton groups have not been adequately defined.

Predicting the activities of planktonic marine microbes is predicated on basic knowledge of the distribution of biomass among the various taxonomic and functional assemblages that comprise these communities because that information helps place constraints on rates of production and turnover. The distribution of particulate organic carbon (POC) among the various microbial assemblages is therefore of fundamental importance for modeling and predicting energy utilization and carbon flow in the plankton. Unfortunately, defining these carbon budgets has been difficult. This situation is due, in part, to the fact that most studies of planktonic microbial communities have focused only on specific components of the community (often only the phytoplankton or bacteria) and, in part, because of uncertainties associated with converting cell abundances to standing stocks of carbon or major nutrients. Obtaining more complete data of microbial abundances has been addressed by the development and application of a suite of methodologies that now allow relatively thorough characterization of all major groups of microbes in a sample, yet conversion to biomass remains problematic.

Most past studies that have reported abundances and biomass across many microbial taxa have been conducted on plankton communities of open ocean environments, and often within the context of major oceanographic programs such as the Joint Global Ocean Flux Study (JGOFS) or in conjunction with oceanic time series stations (Caron et al., 1995; Roman et al., 1995; Buck et al., 1996; Stoecker et al., 1996; Garrison et al., 2000; Dennett et al., 2001; Steinberg et al., 2001; Brown et al., 2003; Church et al., 2010; Karl and Church, 2014). Reports prior to the mid-1990s did not include viruses whose potentially important contribution to POC was not yet realized, or the contribution of mesozooplankton in some cases. Those studies clearly demonstrated the considerable contribution of heterotrophic microbes to the total standing stock of living biomass in the plankton, and in particular the importance of heterotrophic bacteria (including bacteria + archaea; henceforth referred to as 'bacteria'). However, studies examining the distribution of plankton biomass among the various microbial taxonomic groups are rare from coastal ecosystems because such analyses have not been a priority for most coastal studies. Nevertheless, these regions can be important sinks for atmospheric carbon dioxide (Hales et al., 2005), and it is therefore imperative to fully characterize and understand the abundances, biomasses and activities of the plankton assemblages in these regions.

A 3-year dataset of microbial abundances and biomass, and supporting chemical/physical data collected at the San Pedro Ocean Time-series (SPOT) site off southern California, USA, was analyzed in order to determine and compare the monthly and seasonal variability in standing stocks of various planktonic taxonomic groups (viruses to mesozooplankton). Previous studies conducted at the site have documented vertical, monthly, seasonal, annual and interannual changes in species richness and community composition of the microbial assemblages, as well as trophic relationships and associations among these microbial groups (Fuhrman et al., 2009; Schnetzer et al., 2011; Steele et al., 2011; Chow and Fuhrman, 2012; Chow et al., 2013, 2014; Kim et al., 2013; Cram et al., 2014). The present study was conducted to provide these investigations with contextual information on the overall abundances and biomasses of the various microbial groups, and a framework for examining trophic interactions and carbon flow through this planktonic community (Connell et al., In preparation).

Summed across all years and months, integrated microbial biomass in the upper 100 m of the water column was approximately 4 g C m^{-2}, with heterotrophs constituting approximately half of that biomass (predominantly bacteria, but also significant contributions of heterotrophic protists). Minute (< 2 μm) cyanobacteria and eukaryotic algae generally dominated the biomass of phototrophs in the euphotic zone where they were approximately one quarter of the total microbial biomass, but diatoms were seasonally important. Mesozooplankton contributed a minor overall component to total plankton biomass (≈0 to a maximum of < 10% seasonally).

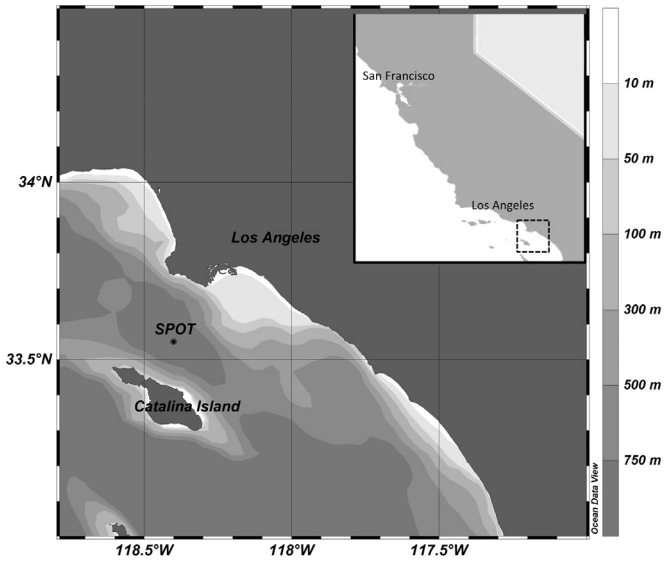

Fig. 1. Location of the San Pedro Ocean Time-series site off the coast of southern California, USA.

2. Materials and methods

2.1. Study area, environmental parameters

The San Pedro Ocean Time-series (SPOT) site is situated centrally in the San Pedro Basin approximately 15 km from the coast of southern California (33°33' N; 118°24' W), USA, between the highly urbanized region of greater Los Angeles and the relatively undeveloped Santa Catalina Island (Fig. 1). The basin has a water depth at the sampling site of ≈890 m, and sills occur to the east and west at water depths of approximately 740 and 650 m, respectively. Water flow through the basin is limited by this bottom topography, and the water column below approximately 300 m persistently experiences < 1 ml l^{-1} oxygen.

Water column sampling and chemical/physical measurements were conducted aboard the R/V Sea Watch using a rosette sampler equipped with an array of sensors and Niskin bottles for water collection. Samples and water column properties were collected approximately monthly as a part of the San Pedro Oceanographic Time-series Program. Details and chemical/physical data are available through the SPOT website (http://dornsife.usc.edu/spot/ctd-data/). Measurements of temperature and depth were accomplished with a Sea-bird Electronics or SBE 911 plus CTD (Sea-Bird Electronics, Inc., Bellevue, WA, USA), in situ chlorophyll fluorescence was measured using a Wet Labs WETStar fluorometer (WETLabs, Philomath, OR, USA) or Seapoint fluorometer (Seapoint Sensors, Inc., Exeter, NH, USA) and dissolved oxygen was measured with a SBE 13 sensor (Sea-Bird Electronics, Inc.), attached to the water-sampling rosette.

Measurements of dissolved oxygen and nutrients (nitrate, nitrite, phosphate and silicate) were obtained from samples collected in Niskin bottles on the rosette. Samples were generally collected and processed from 12 depths in the upper 500 m. Dissolved oxygen concentrations were measured by Winkler titration (Grasshoff et al., 2007), while nutrient concentrations were measured using an Alpkem RFA Auto Analyzer (Alpkem Corporation, Clackamas, OR) using standard proto-

cols (Gordon et al., 1993). The latter measurements were performed by SPOT personnel and are available through the SPOT website. Mixed-layer depths (MLDs) of the water column were defined and calculated for each cruise as in Kim et al. (2013), as the depths at which σ_θ (potential density) differed from surface water (10 m) σ_θ by 0.125 kg m^{-3} (Levitus, 1982).

2.2. Collecting and counting plankton assemblages

A three-year dataset (2000–2003) of monthly samples collected at four depths was analyzed for all components of the microbial planktonic community (viruses to protistan microplankton), as described below. A two-year dataset during the same time period was collected and analyzed for mesozooplankton (metazoan > 200 μm). Water samples from the Niskin bottles were processed for the determination of abundances of viruses, heterotrophic bacteria (including bacteria + archaea; henceforth referred to as 'bacteria'), coccoid cyanobacteria (*Synechococcus* spp. and *Prochlorococcus* spp.), phototrophic picoeukaryotes (eukaryotic algae < 2 μm), phototrophic (including mixotrophic) and heterotrophic nanoplankton (2–20 μm), and phototrophic and heterotrophic microplankton (20–200 μm). Sampling depths for determinations of microbial abundances and biomass were 5 m, the depth of the subsurface maximum in chlorophyll concentration (Subsurface Chlorophyll Maximum [SCM], a persistent feature at the SPOT station), 150 m and 500 m. The depth of the SCM was determined on each cruise from real-time chlorophyll fluorescence detected during the vertical profiling with the sampling rosette. Chlorophyll *a* concentrations from 5 m and the SCM were measured on discrete samples collected at these depths and filtered onto GF/F Whatman filters, extracted in 90% acetone for 24 h at −20 °C, and analyzed by standard fluorometric procedures (Parsons et al., 1984).

Samples for virus counts were collected and preserved with 0.02 μm filtered 2% formalin. Viruses were visualized by staining with SYBR Green I (Molecular Probes–Invitrogen) and counted by epifluorescence microscopy (Noble and Fuhrman, 1998). Samples for the enumeration of heterotrophic bacteria, *Synechococcus* spp., *Prochlorococcus* spp. and phototrophic picoeukaryotes were preserved with 1% filtered formalin and stored frozen at −80 °C until analyzed by flow cytometry. Flow cytometry was conducted using a FACSCalibur flow cytometer (Becton Dickinson). Cyanobacteria and picoplanktonic eukaryotic algae were detected by the autofluorescence of photosynthetic pigments and forward scatter, while bacterial abundances were determined by staining samples with SYTO 13 to visualize them and counted using a routine protocol by flow cytometry (del Giorgio et al., 1996).

Samples (100 ml) for nanoplankton counts (phototrophic and heterotrophic protists 2–20 μm in size) were preserved with 1% filtered formalin and stored at 4 ° in the dark until processing (generally within 24 h). Subsamples of 25–50 ml were stained with 4',6-diamidino-2-phenylindole (DAPI; 25 mg ml^{-1} final concentration), filtered onto 0.8-μm black polycarbonate filters and counted by epifluorescence microscopy using standard methods (Sherr et al., 1993). Phototrophic and heterotrophic forms were distinguished based on the presence or absence of chlorophyll autofluorescence. Mixotrophic forms (phagotrophic phytoflagellates capable of ingesting prey) were not distinguished and therefore were included in the counts of phototrophic nanoplankton (Sanders and Porter, 1988). Microplankton (predominantly protists 20–200 μm in size) were preserved with 10% Lugol's solution (250 ml in amber glass bottles, stored in a cool darkened room until counted), and counted by settling 80–100 ml subsamples in settling chambers and analyzing by inverted light microscopy. Lugol's solution allowed better visualization and enumeration of some taxa (Utermöhl, 1958), but dinoflagellates were not distinguished as phototrophs or heterotrophs in the microscopical counts because Lugol's solution masks the autofluorescence of chlorophyll. Additionally, as a group, dinoflagellate nutrition is complex including obligate heterotrophs, phototrophs and many mixotrophs. A detailed taxonomic characterization of the dinoflagellates was beyond the scope of this study and therefore half of the dinoflagellates were assumed to be phototrophic and half were assumed to be heterotrophic (Sherr and Sherr, 2007). Distinctions among major groups of microplankton (diatoms, dinoflagellates, ciliates) were made at 200× or 400× magnification on an inverted microscope.

Mesozooplankton samples (metazoa > 200 μm) were collected using a 50 cm diameter 200 μm mesh, Sea-Gear® model 9000 plankton net. Oblique tows in the top 100 m of the water column were conducted. Nets were towed at ≈30 cm per second, continuously lowered and raised to provide a single depth-integrated sample. The volume filtered was estimated using a Sea-Gear mechanical impeller flow meter calibrated according to the manufacturers specifications. All tows were conducted during daylight hours (10:00–14:00 h). Total zooplankton displacement volume was determined for each sample from the net tow material using standard protocols (Wiebe et al., 1975), and major taxonomic groups of zooplankton were determined using a dissecting microscope.

2.3. Estimating biomass of plankton assemblages

Abundances of each plankton assemblage described above were converted to particulate organic carbon (POC) using approaches and conversion factors chosen from the literature that were representative of coastal ocean microbes (Table 1). Viruses were converted assuming an average value of 0.2 fg C $virus^{-1}$ (Kepner et al., 1998; Suttle, 2005). Bacteria were converted directly from cell abundances based on a value of 15 fg C $cell^{-1}$. This value is at the lower end of values derived for coastal regions but higher than some values for oceanic ecosystems (Fukuda et al., 1998; Kawasaki et al., 2011; Buitenhuis et al., 2012). Cyanobacteria (*Synechococcus* and *Prochlorococcus*) were converted to POC assuming values of 200 fg C $cell^{-1}$ and 90 fg C $cell^{-1}$, respectively (Buitenhuis et al., 2012; Martiny et al., 2016). Phototrophic picoeukaryote abundances were converted assuming an average cell diameter of 2 μm, and converting cell volume to carbon based on the value 183 fg C μm^{-3} (Caron et al., 1995). The resulting

Table 1
Carbon conversion factors used in this study for each planktonic assemblage.

Component	Values	Descriptor	References
Viruses	0.2 fg C $virus^{-1}$	Determined empirically	Kepner et al. (1998) Suttle (2005)
Bacteria	15 fg C $cell^{-1}$	Sargasso Sea, oceanic	Caron et al. (1995)
Synechococcus	200 fg C $cell^{-1}$	Sargasso Sea, oceanic	Caron et al. (1995)
Prochlorococcus	90 fg C $cell^{-1}$	S. California, coastal	Martiny et al. (2016)
		Sargasso Sea, oceanic	Casey et al. (2013)
Picoeukaryotes	183 fg C μm^{-3}, assumes average radius of 1 μm	Sargasso Sea, oceanic	Caron et al. (1995)
Nanoflagellates	183 fg C μm^{-3}, assumes average radius of 1.5 μm	Sargasso Sea, oceanic	Caron et al. (1995)
Microplankton	138 pg C $cell^{-1}$	Sargasso Sea, oceanic	Caron et al. (1995)
Mesozooplankton	21 mg C cm^{-3}	NW Spain, coastal (based on displacement volume)	Bode et al. (1998)

carbon content is within the range but at the lower end of published values for this assemblage (Buitenhuis et al., 2012; Casey et al., 2013). Our flow cytometric counting approach for phototrophic picoeukaryotes (< 2 μm) was designed to minimize overlap with microscopical counts of nanoplankton, the latter were converted assuming an average cell diameter of 3 μm and the same conversion factor (183 fg C μm^{-3}). Microplankton cells were converted to POC based on a constrained conversion value (138 pg C $cell^{-1}$) derived by Caron et al. (Caron et al., 1995). Mesozooplankton displacement volumes (Wiebe et al., 1975) were converted to POC based on a conversion factor of 21 mg C ml^{-1}, representative of a mixed zooplankton assemblage (Bode et al., 1998; Harris et al., 2000) (Table 1).

Depth-integrated carbon biomass of the plankton community (0–100 m and 0–500 m) was obtained from the biomass measured at each of the four depths multiplied by the interpolated depth ranges between the sampling depths. Depth ranges between the 5 m and SCM, and the SCM and 150 m varied due to the variability of the depth of the SCM. Integrated biomass values between the surface and 500 m were estimated as the sum of biomass in each depth interval (as POC m^{-2}) using the following equation: [(5+(SCM-5)/2)×(5 m biomass values)] +[((SCM-5)/2+(150-SCM)/2)×(SCM biomass values)] +[((150-SCM)/2+(500-150)/2)×(150 m biomass values)] +[((500-150)/2)×(500 m biomass values)]. Integrated biomass values between the surface and 100 m were estimated as follows: [(5+(SCM-5)/2)×(5 m biomass values)] +[((SCM-5)/2+(150-SCM)/2)×(SCM biomass values)] +[(100-((5+(SCM-5)/2)+(SCM-5)/2+(150-SCM)/2))×(150 m biomass values)].

Monthly averages of carbon biomass were determined from values in each month collected throughout the three-year study. Seasonal averages were then determined for the months December-February (winter), March-May (spring), June-August (summer) and September-November (fall).

3. Results

3.1. Hydrography and oceanographic context

The hydrography and environmental parameters at our study site in the central San Pedro Basin have been previously detailed (Berelson, 1991; Countway et al., 2010; Beman et al., 2011; Collins et al., 2011; Hamersley et al., 2011; Schnetzer et al., 2011; Chow and Fuhrman, 2012; Kim et al., 2013; Cram et al., 2014). Representative vertical profiles of pertinent parameters from four seasons during this study illustrate a persistently-stratified water column with considerable vertical structure (Fig. 2). Seasonal temperatures at the surface fluctuated approximately 5–6 °C, with a typical seasonal low of 14 °C and a seasonal high of 19–20 °C (Fig. 2a). Water temperature below approximately 40 m decreased from 11 to ≈6 °C at 500 m regardless of season (inset in Fig. 2a). A similar pattern of decreasing concentrations of dissolved oxygen with depth was observed, although oxygen decreased more gradually than temperature (Fig. 2b). Water at our sampling depth of 500 m contained persistently low concentrations of dissolved oxygen (< 1 ml l^{-1}), indicative of restricted flow into and out of the basin. Our sampling depth of 150 m exhibited dissolved oxygen concentrations that were relatively constant at approximately half surface values.

Nutrient patterns indicated that productivity in surface waters at the study site were typically and consistently N-limited (Fig. 2c-f). Nitrate was near or below the analytical limit of detection at all seasons, although nitrite showed a pronounced peak in concentration at approximately 40 m (within the region of rapidly decreasing dissolved oxygen concentrations). Phosphate and silicate concentrations were substantially lower in surface waters than at depth, but were generally detectable in all seasons (insets in Fig. 2e,f).

Monthly changes in the average mixed layer depth during the three-year study indicated a relatively shallow mixed layer throughout much of the year at the SPOT study site (Fig. 3). Mixed layers in spring through fall were generally < 20 m, while mixed layers during the winter occasionally exceeded 40 m. The year round persistence of well-defined mixed layers is indicative of the subtropical climate of the region.

The existence of a relatively shallow mixed layer throughout the year at the SPOT site resulted in the development and maintenance of a modest but persistent subsurface maximum in chlorophyll concentration (Subsurface Chlorophyll Maximum: SCM) that always equaled or exceeded chlorophyll concentrations observed near the surface, with the exception of September 2002 (Fig. 4). The depth and magnitude of the SCM varied seasonally but rarely exceeded ≈2 μg l^{-1} throughout the three-year study period. Differences in chlorophyll concentrations between the two depths were typically more pronounced during summer months than winter. This pattern is consistent with trends observed at the sampling site across a 10-year period (Chow et al., 2013; Kim et al., 2013).

3.2. Microbial abundances at the San Pedro Ocean Time-series station

Abundances of the various microbial assemblages observed at four depths in the water column at the SPOT study site varied by seven orders of magnitude (Table 2). Viral particles were the most abundant assemblage, exceeding 10^7 particles ml^{-1} in surface waters, with abundances approximately one order of magnitude lower at 500 m. Bacteria were approximately 10-fold less abundant than viruses (average ≈2×10^6 ml^{-1} in the mixed layer) and also decreased one order of magnitude with depth. Abundances of coccoid cyanobacteria (*Synechococcus* spp. and *Prochlorococcus* spp.) were ≈$1–3\times10^4$ ml^{-1} in mixed layer samples, with *Synechococcus* generally twice as abundant as *Prochlorococcus*, while phototrophic picoeukaryotic algae were 2–3-fold less abundant than cyanobacteria (averages of ≈0.9–1×10^4 ml^{-1}). These three latter phototrophic assemblages were largely relegated to samples collected at 5 m and the SCM (values were > 2 orders of magnitude lower at 150 and 500 m).

Protists > 2 μm in size occurred at significantly lower abundances than prokaryotic assemblages. Phototrophic/mixotrophic and heterotrophic nanoplankton (P/MNANO and HNANO) occurred at average abundances of 0.8–3×10^3 ml^{-1} in samples from the mixed layer, with HNANO abundances generally 2–3× the abundances of P/MNANO. P/MNANO abundances decreased precipitously with depth, while decreases in HNANO were > 10-fold. Microplanktonic protists (> 20 μm in size; predominantly ciliates, dinoflagellates and diatoms) were present at averages of a few to 10 s cells ml^{-1} in samples from the mixed layer. Ciliate abundances were > 10-fold lower in deep samples at the site, while dinoflagellates and diatoms at 150 and 500 m only decreased by approximately half their abundances relative to samples from the mixed layer. The presence of dinoflagellates in deep waters at the SPOT site may reflect shifts in species composition of this assemblage from phototrophic to heterotrophic taxa, while the existence of diatoms in deep samples presumably reflected rapid sinking of these phototrophic cells from surface waters (Schnetzer et al., 2007).

All of the microbial assemblages varied with sampling season (note ranges in abundances in Table 2 below mean values). These variances in abundance were reflected in their contributions to overall microbial biomass at the study site (see below).

3.3. Total microbial biomass

The large differences in microbial abundances observed at the SPOT site were dramatically reduced when the biomass of each assemblage was estimated from cell abundances and appropriate conversion factors (Fig. 5). Integration of microbial biomass to 100 m was used because it approximates the lower-most extent of the seasonally-independent thermocline and nutricline, and therefore

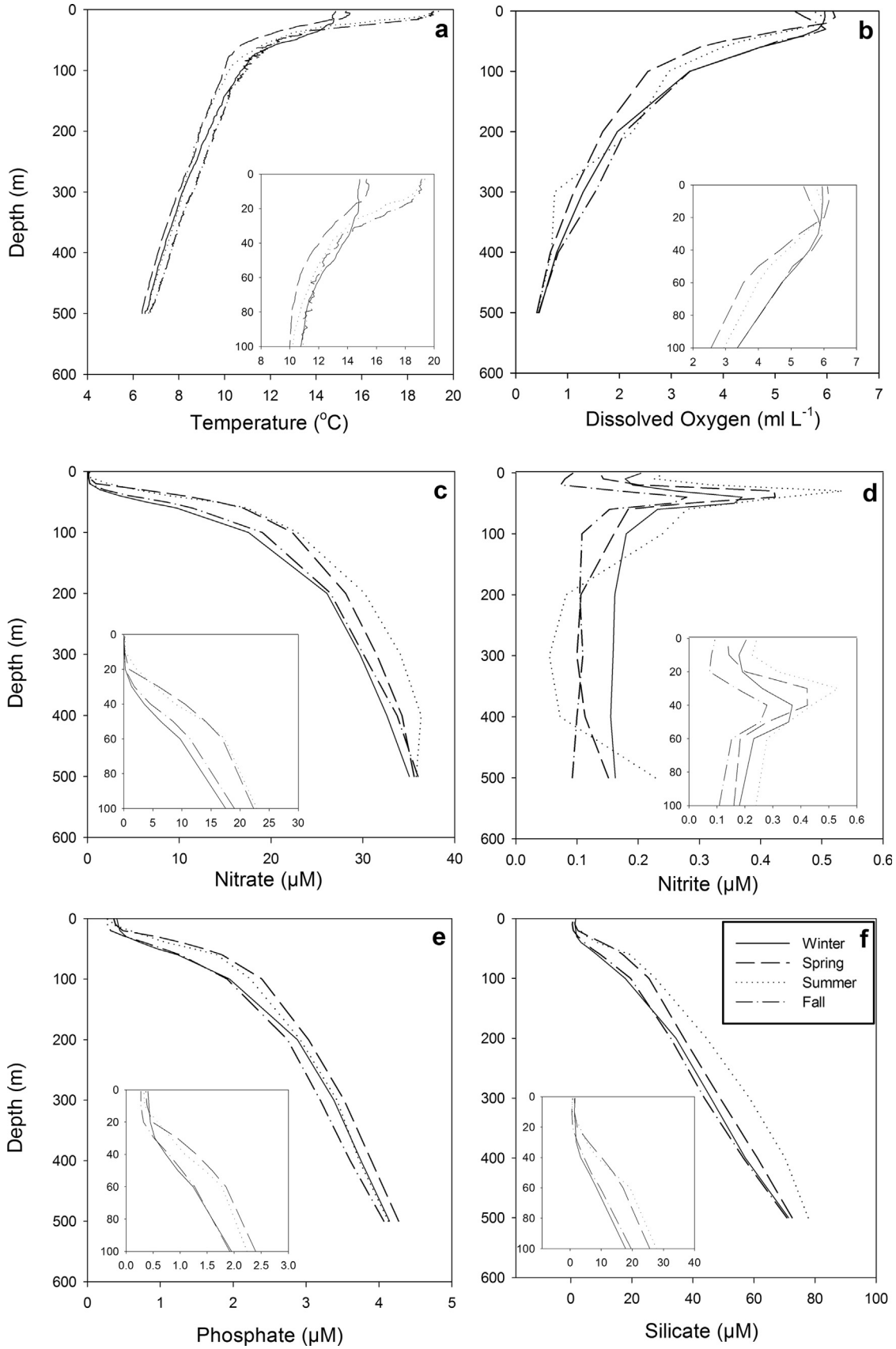

Fig. 2. Vertical profiles of chemical and physical parameters in the top 500 m at the San Pedro Ocean Time-series sampling site: (a) temperature; (b) dissolved oxygen; (c) nitrate concentration; (d) nitrite concentration; (e) phosphate concentration; (f) silicate concentration. Representative profiles from four seasons are shown. Insets show expanded data in the top 100 m of the water column.

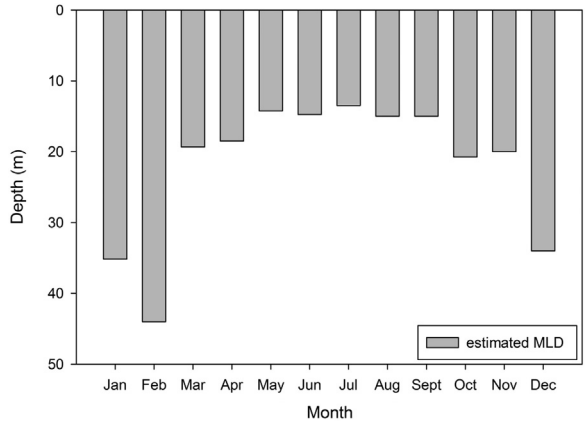

Fig. 3. Mixed layer depths measured at the site of the San Pedro Ocean Time-series.

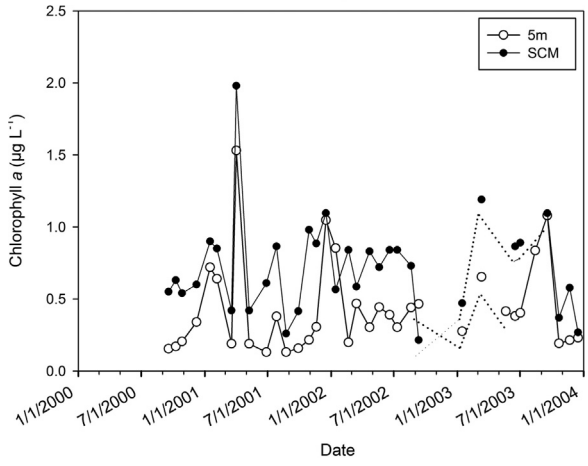

Fig. 4. Chlorophyll *a* concentrations measured at 5 m and at the depth of the subsurface chlorophyll maximum (SCM), at the site of the San Pedro Ocean Time-series.

represents a reasonable approximation of plankton standing stocks in the water column directly influenced by near-surface processes (Fig. 2, and data not shown). Bacteria constituted nearly one third of the total microbial biomass when integrated throughout the top 100 m of the water column (Fig. 5a), and made a somewhat larger contribution to total biomass when integrated over 500 m due to reduced contributions by most phototrophic components (Fig. 5b). Phototrophic prokaryotes (*Synechococcus* and *Prochlorococcus*) and eukaryote algae < 2 µm in size comprised approximately one quarter of the microbial biomass in the top 100 m, but only half that value when biomass was integrated for the upper 500 m.

All protists (pico-, nano- and microplanktonic phototrophs and heterotrophs) totaled > 40% of the microbial biomass at the SPOT site, and were very similar for the two depth integrations (Fig. 5a,b). Reductions in the contributions of phototrophic picoeukaryote and P/MNANO assemblages in the 0–500 m integration relative to the 0–100 m integration were offset by greater relative contributions of dinoflagellates and diatoms in deep samples.

Despite their numerical dominance in the water column relative to all other microbial assemblages (Table 2), viruses comprised < 10% of total microbial biomass, and their contribution was relatively unchanged for the 0–100 and 0–500 m depth integrations (Fig. 5a,b). Depth-integrated biomass of all microbial assemblages in the top 100 m of the water column was ≈4 g C m^{-2}, approximately half the biomass estimated in the top 500 m of the water column (Fig. 5c).

Carbon-to-chlorophyll ratios (C:Chl: by mass) were calculated for samples obtained from 5 m and the SCM using carbon values estimated from cell abundances for phototrophic assemblages and their group-

Table 2
Mean annual cell abundances at each depth for the major microbial groups observed at the site of the San Pedro Ocean Time-series.

	VIRUS	BACT	SYN	PRO	PEUK	P/MNANO	HNANO	CIL	DINO	DIAT
Cells ml^{-1}	10^7	10^6	10^4	10^4	10^3	10^3	10^3			
5 m										
x̄ (± s)	2.6 (± 2.0)	1.5 (± 0.98)	2.3 (± 2.2)	1.5 (± 1.6)	9.3 (± 15)	0.76 (± 0.67)	3.1 (± 3.7)	6.3 (± 5.8)	8.2 (± 6.4)	43 (± 51)
Range	0.32–10	0.36–4.1	0.17–9.2	0.0081–6.9	0.055–74	0–2.4	0.70–22	0–27	0–30	0–210
SCM										
x̄ (± s)	2.3 (± 1.8)	1.5 (± 0.82)	2.7 (± 3.6)	1.3 (± 1.7)	9.8 (± 10)	1.2 (± 0.83)	2.3 (± 1.7)	9.8 (± 8.8)	11 (± 10)	32 (± 32)
Range	0.26–10	0.38–3.8	0.20–12.9	0.077–8.3	2.1–38	0.14–3.4	0.34–7.9	0.8–40	0–36	0.8–120
150 m										
x̄ (± s)	0.45 (± 0.25)	0.32 (± 0.16)	0.011 (± 0.062)	0.023 (± 0.023)	0.079 (± 0.072)	0.00017 (± 0.00090)	0.10 (± 0.043)	0.55 (± 0.45)	3.5 (± 5.9)	17 (± 26)
Range	0.038–1.2	0.12–0.90	0.0030–0.026	0–0.11	0.006–0.39	0–0.0050	0.024–0.19	0–1.5	0–25	0.5–100
500 m										
x̄ (± s)	0.22 (± 0.08)	0.19 (± 0.067)	0.0064 (± 0.054)	0.021 (± 0.021)	0.036 (± 0.029)	0 (± 0)	0.069 (± 0.036)	0.21 (± 0.28)	3.0 (± 5.7)	20 (± 35)
Range	0.090–0.42	0.074–0.33	0.00050–0.028	0–0.071	0–0.11	0–0	0.029–0.18	0–0.90	0–26	0–190

Abundances are averages ± 1 standard deviation, and overall ranges (cells ml^{-1}) for all samples from the three-year time series. Headings indicate viruses (VIRUS), heterotrophic bacteria + archaea (BACT), *Synechococcus* (SYN), *Prochlorococcus* (PRO), picoplanktonic phototrophic eukaryotes (PEUK), phototrophic/mixotrophic nanoplankton (P/MNANO), heterotrophic nanoplankton (HNANO), ciliates (CIL), dinoflagellates (DINO) and diatoms (DIAT).

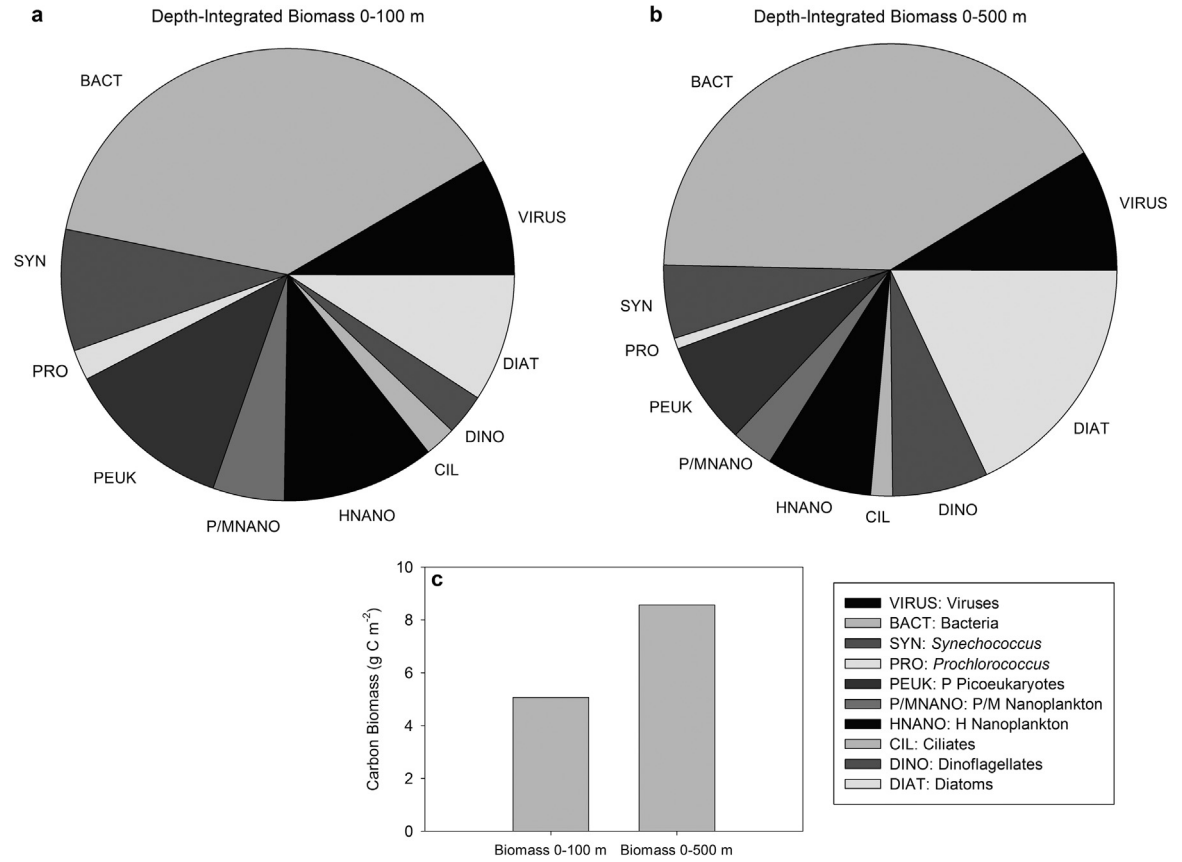

Fig. 5. Contributions of the various microbial assemblages (as percent of total microbial carbon) to depth-integrated microbial biomass at 0–100 m (a) and 0–500 m (b) at the San Pedro Ocean Time-series site. (c) Total depth-integrated organic carbon (μg C m^{-2}) summed across all microbial assemblages for 0–100 and 0–500 m.

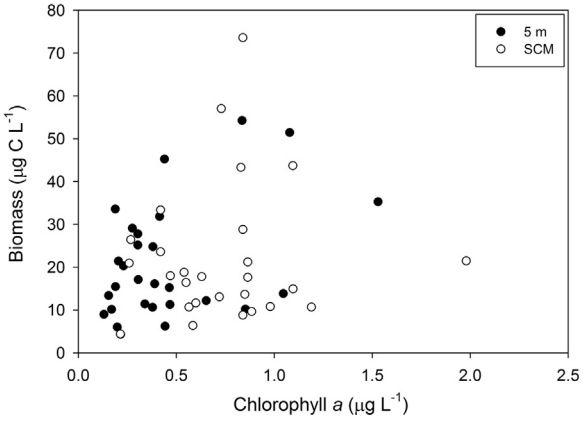

Fig. 6. Scatter plot of carbon contained in phototrophic microbes relative to the chlorophyll *a* concentrations in those samples for all samples collected throughout the 3-year time series at 5 m (solid circles) and at the depth of the subsurface chlorophyll maximum (SCM; open circles). Carbon in the phototrophic microbes was obtained by summing the carbon content estimated for the *Synechococcus*, *Prochlorococcus*, phototrophic picoeukaryote, phototrophic/mixotrophic nanoplankton, and microplanktonic phototroph assemblages.

specific conversion values, and chlorophyll values measured fluorometrically in the same samples. C:Chl ratios were calculated using the combined biomass of the cyanobacteria, phototrophic picoeukaryotes, P/MNANO, and microplanktonic phototrophs; (Fig. 6). These ratios provide a degree of evaluation of the conversion factors used to estimate organic carbon for phototrophic microbial groups (see Materials and methods; also see Caron et al. (1995) for reasoning). Ratios obtained for samples analyzed in the study were highly variable (Fig. 6). The average C:Chl ratio for samples collected at 5 m was 57, while samples collected at the SCM yielded an average C:Chl of 34. These averages are well within the range of values reported in the literature for surface-dwelling and low-light adapted phytoplankton assemblages, respectively.

3.4. Vertical and seasonal variances in microbial biomass

The vertical distribution of microbial biomass at the SPOT site reflected absolute reductions in the biomass of all microbial assemblages with depth (Fig. 7). Total microbial biomass ranged from nearly 60 μg C l^{-1} at 5 m to < 10 μg C l^{-1} at 500 m. Contributions of the various assemblages to microbial biomass were relatively consistent for samples from 5 m and the SCM, as well as for samples from 150 and

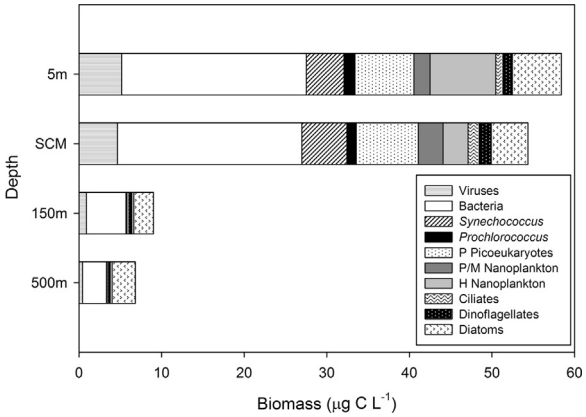

Fig. 7. Three-year average of the distribution of carbon (μg C l^{-1}) contained in various microbial assemblages at 5 m, the depth of the subsurface chlorophyll maximum (SCM), 150 m and 500 m at the site of the San Pedro Ocean Time-series.

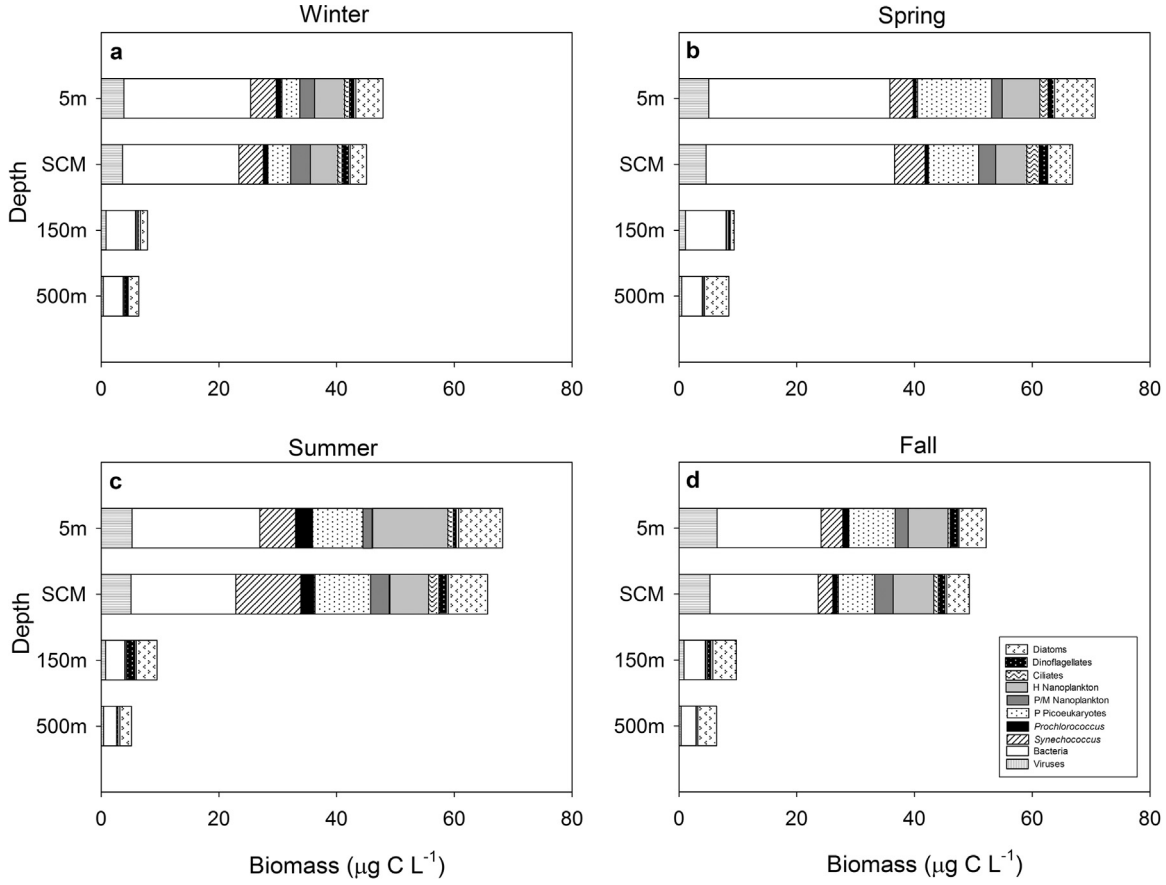

Fig. 8. Seasonal averages in the distribution of carbon (μg C l^{-1}) contained in various microbial assemblages at 5 m, the depth of the subsurface chlorophyll maximum (SCM), 150 m and 500 m at the site of the San Pedro Ocean Time-series. Data were averaged for each season across the 3-year time series for (a) winter, (b) spring, (c) summer and (d) fall.

500 m, but samples from the upper water column had more than 5 times greater biomass than the two deep samples (Fig. 7). Seasonal fluctuations in the vertical distribution of microbial biomass were not dramatic (Fig. 8). Values at 5 m and the SCM observed during spring and summer were greater than values observed at those depths during winter and fall (Fig. 8b,c vs. 8a,d, respectively), but only modestly so (approximately 40% greater). Biomass at 150 and 500 m remained relatively unchanged seasonally.

Microbial biomass estimated for samples collected at 5 m and the SCM averaged over the three-year study period exhibited more variability monthly (Fig. 9a,b) than seasonally (Fig. 10a,b). A similar relationship was observed for depth-integrated microbial biomass (Fig. 9c,d vs. 10c,d). Monthly values varied as much as 2–3× while seasonal averages varied by 30–40%. Among the monthly estimations, April (with one exception) was generally a period of particularly high standing stocks of microbial biomass (Fig. 9).

3.5. Mesozooplankton contribution to plankton community biomass

The contribution of mesozooplankton biomass, estimated directly from measurements of displacement volume for two years of monthly samples, revealed a single large peak in biomass during late spring and early summer (Fig. 11a). Mesozooplankton contributed < 1 μg C l^{-1} during late winter, and a maximum of 6.3 μg C l^{-1} at peak contribution. Qualitative information on the composition of the mesozooplankton assemblage was obtained by microscopy on these samples. All samples were strongly dominated by crustaceans (predominantly calanoid copepods) numerically, and copepods also contributed a dominant fraction of the total displacement volumes. Appendicularia, chaetognaths and small cnidaria made minor but relatively consistent contributions.

Mesozooplankton biomass always constituted a minor component of total biomass when compared to either microbial prokaryotic or microbial protistan biomass (Fig. 11b), although mesozooplankton may have been underestimated in this study because all net tows were performed during the day, and therefore did not assess the importance of nighttime vertical migrators. Only in one sample, when mesozooplankton biomass was maximal (June), did these species contribute 10% of the total microbial biomass.

4. Discussion

Climate change is expected to alter water column physics and chemistry of coastal ecosystems in the coming decades. The details of these changes and their impacts on pelagic food web structure and function in many locations is still being debated (Sydeman et al., 2014), but the impact of shifting climate has already been documented for important fisheries species at the top of some marine food webs (Cheung et al., 2013). The consequences of such environmental change on planktonic assemblages comprising the base of the food web are less well characterized but are essential for understanding how climate change will affect energy production and overall food web structure (Hofmann et al., 2013).

Towards this end, benchmark information derived from long-term marine observing programs in oceanic realms have provided unique perspectives on the multi-decadal response of pelagic oceanic communities and biogeochemical processes to climatological forcing (Karl and Michaels, 1996; Steinberg et al., 2001; Karl and Church, 2014). Time-series observatories in coastal ecosystems have more recently begun to contribute insight (Alber et al., 2013). For example, analysis of satellite data along the west coast of the U.S. has indicated that phytoplankton standing stocks within the California Current System, and more locally phytoplankton

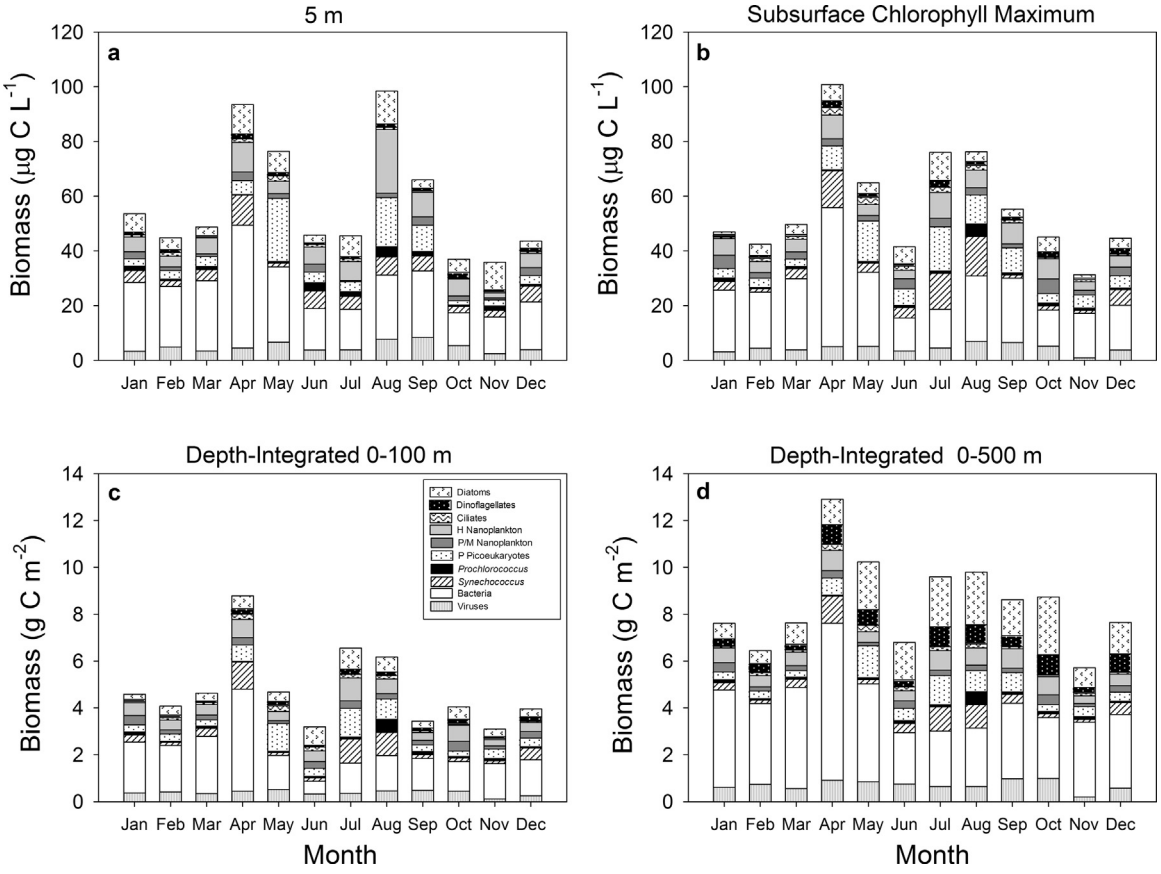

Fig. 9. Monthly averages in the distribution of carbon among the various microbial assemblages throughout the 3-year time series at the San Pedro Ocean Time-series site. Organic carbon (µg C l^{-1}) estimated at 5 m (a) and the depth of the subsurface chlorophyll maximum (SCM (b). Depth-integrated carbon (µg C m^{-2}) for 0–100 m (c) and 0–500 m (d).

bloom events within the Southern California Bight, increased during the period 1997–2007 (Kahru et al., 2009; Nezlin et al., 2012). Conversely, analysis of a multi-decadal time-series of zooplankton throughout the California Cooperative Oceanic Fisheries Investigation grid (CalCOFI) indicated a decline in zooplankton displacement volume that was attributed to decreasing abundances of pelagic tunicates (Lavaniegos and Ohman, 2007). Such changes may be due to influences on upwelling frequency or severity (Aksnes and Ohman, 2009; Rykaczewski and Dunne, 2010), since coastal upwelling appears to be the primary driver of production in the Bight region. Additionally, the contribution of high-nutrient effluent discharge from Publicly Owned Treatment Works (POTWs) may be significant on smaller, local temporal and spatial scales (Kudela et al., 2005; Howard et al., 2014). Whether these shifts in system productivity represent normal decadal-scale oscillations or anthropogenic effects (either large-scale climatic shifts or local changes in coastal development) is unclear. The lifespans of many coastal observatories are still relatively short and often include a limited number of biological measurements, and are therefore just beginning to provide insight into the long-term responsiveness of these productive and highly utilized (and often impacted) areas of the ocean.

The San Pedro Ocean Time-series has been the site of monthly measurements of ocean chemistry and physics for nearly twenty years. The site has also been the location of fairly extensive observations of microbial oceanography as part of a National Science Foundation Microbial Observatory beginning in 2000, and more recently a NSF Dimensions of Biodiversity project. These programs have supported measurements of planktonic microbial diversity (viruses, archaea, bacteria, microbial eukaryotes), and together constitute one of the longest time series of microbial oceanography at a coastal site. This study presents an analysis of the abundances and standing stocks of biomass of these various microbial assemblages for this site.

4.1. Constraining conversion factors and estimating depth-integrated biomass

The construction of models summarizing microbial biomass and energy flow in pelagic ecosystems is dependent on the ability to count all planktonic microbial groups (viruses, bacteria, etc.), converting cell abundances or cell volumes to carbon biomass (Anderson and Ducklow, 2001), and summing biomass across all groups within the water column. By far, the largest uncertainty in the methodologies applied to derive living biomass in natural microbial communities lies in the conversion factors employed to conduct these studies. While our knowledge of the diversity of planktonic microbes and methods for enumerating them in natural communities have improved significantly in recent years, estimates of their contributions to particulate organic carbon are still affected by often-poorly-constrained conversion factors. Unfortunately, empirical determination of these factors for all plankton compartments in the present study was not realistic, therefore we chose relatively conservative conversion factors to avoid overestimating microbial biomass. Nonetheless, over- or underestimation may have occurred for one or more of the categories examined.

The conversion of bacterial abundances to POC is probably the most poorly constrained parameter when estimating microbial biomass in the plankton. This situation exists because bacterial cell volume is highly variable with taxonomic composition of the assemblage and metabolic state (and very difficult to measure directly), and also because bacteria generally constitute the largest single compartment of living microbial biomass in the plankton within many aquatic ecosystems including the SPOT site (e.g. Figs. 5, 7, 8). A recent review of bacterial conversion factors indicated an overall range of two orders of magnitude; 2–260 fg C $cell^{-1}$ (Kawasaki et al., 2011). These authors used a value of 6.3 fg C $cell^{-1}$ to estimate the amount of living carbon in

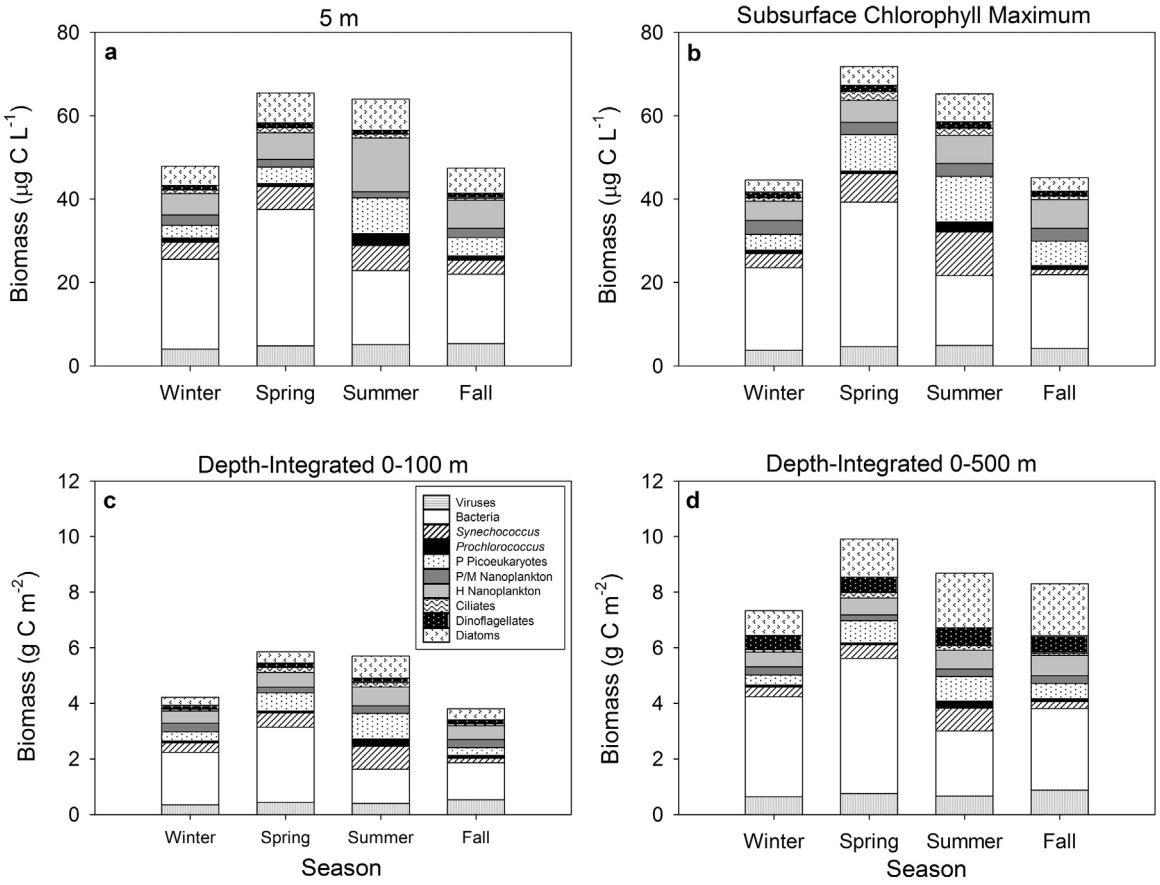

Fig. 10. Seasonal averages in the distribution of carbon among the various microbial assemblages throughout the 3-year time series at the San Pedro Ocean Time-series site. Organic carbon (µg C l^{-1}) estimated at 5 m (a) and the depth of the subsurface chlorophyll maximum (SCM (b). Depth-integrated carbon (µg C m^{-2}) for 0–100 m (c) and 0–500 m (d).

the bacterial assemblage at Station ALOHA in the oligotrophic North Pacific gyre, and noted that the choice of conversion factor significantly affected estimates of the standing stock of bacteria in oceanic regions (nearly 6-fold; see Table 4 in Kawasaki et al. (2011)). A global inventory of oceanic bacterial biomass by Buitenhuis et al. (2010) employed a value of 9.1 fg C $cell^{-1}$. The authors reported that bacterial carbon biomass in much of the world ocean was in the range 10–20 µg C l^{-1}. These latter values are in line with estimates of bacterial biomass observed in the present study (≈20 µg C l^{-1} in samples from the upper water column; Figs. 5a,b, 7, 8).

The conversion factors employed in the studies described above are appropriate for oceanic bacterial assemblages, but carbon $cell^{-1}$ derived for coastal communities of bacteria have typically been much greater than values applied to oceanic environments (Lee and Fuhrman, 1987; Cho and Azam, 1990; Fukuda et al., 1998; Kawasaki et al., 2011). The value of 15 fg C $cell^{-1}$ employed in the present study is on the low end of cellular carbon content reported for coastal marine bacteria, so should represent a reasonably conservative estimate of the contribution of bacteria to total microbial biomass. Our conversion factor is slightly higher than a value (11 fg C $cell^{-1}$) used to estimate bacterial carbon in the Southern California Current System offshore from our study site (Taylor et al., 2015), and therefore seemed appropriate for our coastal station at the edge of that hydrographic region. Use of 11 fg C $cell^{-1}$ for bacteria at the SPOT station would reduce our estimated contribution of bacterial biomass in total microbial carbon in the water column from approximately 40% to approximately 30% (Fig. 5a,b). That estimate would still constitute a dominant component of the living microbial biomass at our study site, but it also indicates the critical nature of one's choice of conversion factor. Unfortunately, factors for converting bacterial abundance to carbon have not become more accurately defined over the last two decades, and therefore they probably comprise the largest single source of uncertainty in estimating living microbial biomass in natural samples.

Conversion factors reported for picoplanktonic phototrophs (*Synechococcus* spp., *Prochlorococcus* spp., phototrophic picoeukaryotes) are also variable, but not to the degree reported for bacteria. The conversion factor that we employed for phototrophic picoeukaryotes (≈770 fg C $cell^{-1}$) represented a conservative estimate for this assemblage based on recent summaries of these values (Buitenhuis et al., 2012; Casey et al., 2013). Similarly, we employed conversion factors for *Synechococcus* and *Prochlorococcus* (200 and 90 fg C $cell^{-1}$, respectively) based on recent reviews of these values (Buitenhuis et al., 2012; Casey et al., 2013) because routine cell sizing was beyond the scope of our study. Our value for *Synechococcus* was an approximate average of the range presented in those reviews, while our conversion factor for *Prochlorococcus* was based on larger cell sizes reported in Veldhuis et al. (1997). Based on our conversion factors, phototrophic picoeukaryotes at our study site contributed a biomass generally equal to or exceeding the biomass of the two cyanobacterial groups (Figs. 5, 7–10). Collectively, the three assemblages averaged approximately 12 µg C l^{-1} in the upper water column (≈20% of total microbial biomass; Fig. 7). Analysis of these three plankton assemblages in the lower Southern California Bight, using somewhat lower conversion values than our study, yielded carbon biomass values that were very similar to our estimates (Worden et al., 2004).

Synechococcus biomass in the present study exceeded that of *Prochlorococcus* by approximately a factor of four (Fig. 5a). A similar result was reported by Worden et al. (2004). However, genetic studies of cyanobacterial diversity conducted at the SPOT site have shown that *Prochlorococcus* sequences are more common than *Synechococcus* sequences in environmental sequence datasets (Chow et al., 2013). That mismatch may be a consequence of an underestimation of the

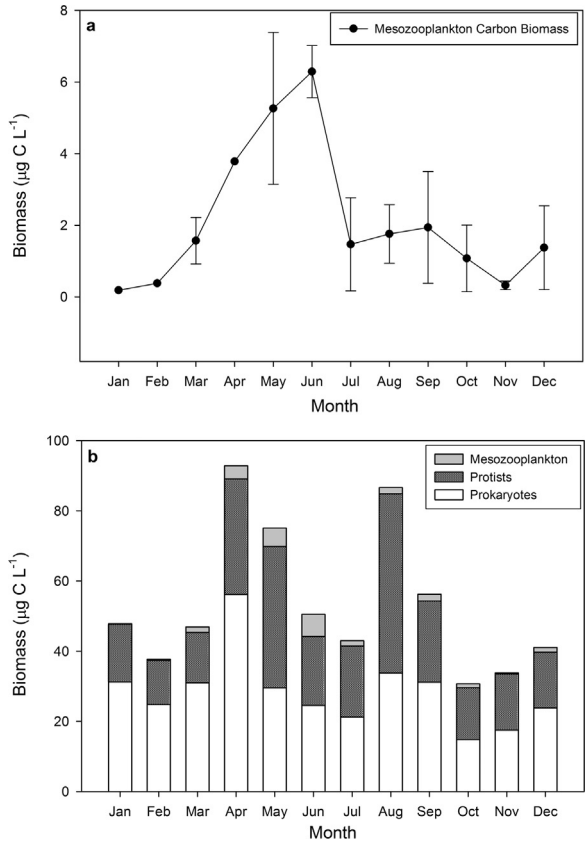

Fig. 11. Monthly averages of mesozooplankton biomass (µg C l^{-1}) over a 2-year period (a), and comparison of mesozooplankton biomass to bacterial (phototrophic and heterotrophic assemblages) and protistan (all protistan compartments) at the San Pedro Ocean Time-series site (b).

abundances of weakly fluorescent *Prochlorococcus* cells by our flow cytometric method, or the use of inappropriate conversion factors for the two groups (although our value for *Prochlorococcus* is already fairly high). Taylor et al. (2015) employed conversion factors that were lower than our values for their offshore communities, and those values were proportionately larger for *Synechococcus* relative to *Prochlorococcus* cell carbon (101 and 32 fg C $cell^{-1}$ for *Synechococcus* and *Prochlorococcus*, respectively). Use of those values would therefore not explain the apparent discrepancy between our molecular diversity findings (Chow et al., 2013) and the cyanobacterial biomass information presented in this study. Conversion factors employed by Martiny et al. (2016) for a coastal study site within the Southern California Bight were more consistent with values employed in our study (120 and 78 fg C $cell^{-1}$ for *Synechococcus* and *Prochlorococcus*, respectively). Regardless of the specific conversion factors used for these assemblages, cyanobacterial biomass constituted a minor percentage of total microbial biomass at the SPOT site (≈12–14%; Figs. 5, 7, 8). Therefore, the use of other factors would result in only minor differences in the overall contribution of cyanobacteria to total microbial biomass.

Nano- and microplankton biomass constituted significant albeit minor fractions of the total microbial biomass at the SPOT site (up to 14% for nanoplankton, < 10% for microplankton; Fig. 5), but were also the least constrained conversion factors in our study. We attempted to choose a conservative value for estimating the contribution of nanoplankton to total microbial biomass (average cell diameter =3 µm, carbon content =183 fg C $µm^3$, yielding a cell carbon content of ≈2.6 pg C $cell^{-1}$). However, data provided on the California Current Ecosystem LTER website (http://oceaninformatics.ucsd.edu/datazoo/data/ccelter/datasets?action=summary&id=57) for samples collected offshore from our study site indicate that a smaller average carbon content might be more appropriate for nanoplankton in the region. Our estimates of nanoplankton biomass were strongly influenced by our estimated cell size. For example, use of an average cell diameter of 2.5 µm rather an 3.0 would reduce our estimate of nanoplankton biomass by nearly 50%. Conversely, increasing the estimated cell size even modestly (e.g. from an average cell diameter of 3–4 µm) would increase the estimated contribution of nanoplankton to total biomass by nearly 2.4-fold. Similarly, a number of relationships have been used to convert protists in the microplankton size range to carbon $cell^{-1}$ (see citations in Menden-Deuer and Lessard (2000)), and our conversion factor (138 pg C $cell^{-1}$) is generally larger than the median value provided for microplankton on the California Current Ecosystem LTER website. However, microplankton biomass did not comprise a major component of the plankton biomass in our study, so small variances presumably would not impose much change on the overall estimation of microbial biomass among the assemblages. An exception may be the diatoms, that have been shown to be significantly less carbon dense than other protistan groups (Menden-Deuer and Lessard, 2000).

One means of constraining conversion factors, or assessing their appropriateness, is to compare values generated from cell abundances and group-specific conversion values with independently measured parameters. We performed such an analysis by calculating C:Chl ratios for the samples collected from 5 m and the SCM. Carbon values were based on the organic carbon contained in all phototrophs (*Synechococcus*, *Prochlorococcus*, picoeukaryotic algae, P/MNANO, and microplanktonic phototrophs) and chlorophyll values were obtained fluorometrically from the same samples. Ratios obtained in this manner for samples from the upper water column (averages of 57 and 34 for 5 m and the SCM, respectively; Fig. 6) were in good agreement with C:Chl values obtained in other studies. Therefore, our estimates of carbon among the microbial phototrophs in our study appear reasonable.

Conversion factors for estimating mesozooplankton carbon content from displacement volume are quite variable (Bode et al., 1998). Mesozooplankton biomass in our study was always a very minor component of the total plankton biomass (Fig. 11b) but our collections were all conducted during daytime hours and therefore must be considered underestimates because they did not take into account the contribution of vertically migrating species that swim into surface waters at night. Nonetheless, mesozooplankton comprised such a small component of the overall carbon biomass in the water column that even a doubling of that value would still constitute only a minor fractional change in our estimate of the biomass of the planktonic community.

Caveats relating to microbial carbon conversion factors place qualifiers on the contribution of the various plankton assemblages to total microbial biomass as noted above. Similarly, our estimations of total microbial biomass integrated throughout the water column (0–100 m and 0–500 m) were influenced by the number of depths for which data were available, and our method of depth integration. The present study encompassed four sampling depths which were chosen to best assess biological assemblages in the upper water column (5 m and the depth of SCM) and the deeper water column (150 m situated within the permanent oxycline, and 500 m to represent the deep water community). Plankton biomasses estimated for the two depths above the permanent thermocline and the two below that layer were similar to each other, but the upper water column and lower water column differed considerably (Figs. 7, 8). We integrated microbial biomass from 0 to 100 m in this study (Figs. 5a, 9c, 10c) because 100 m was a reasonable approximation of the bottom of the permanent thermocline (Fig. 2a). Given differences in the microbial biomass between the upper water column and below the thermocline, our choice of the boundary between the SCM and 150 m samples) was the single largest source of variability when estimating integrated biomass. We divided the water column between the depth of the SCM and 150 m equally in our analysis when determining integrated microbial biomass, which may

have exaggerated the importance of the SCM biomass values in the resulting integrations, particularly for the 0–100 m integration. We estimate that our approach may have yielded values 10–20% higher than a more conservative integration (data not shown).

4.2. The biological structure of the plankton community at the SPOT site

Studies conducted more than two decades ago established that small microbes (picoplankton; cell size < 2 μm) made up a significant portion of the total living biomass of marine plankton communities (Cho and Azam, 1990; Li et al., 1992; Caron et al., 1995; Roman et al., 1995; Buck et al., 1996; Garrison et al., 2000). Those studies established that bacteria, cyanobacteria and some eukaryotes dominate the biomass of larger protists and zooplankton. Most of that work was carried out in order to characterize the standing stocks of organic carbon in relatively large, oligotrophic oceanic provinces where the contribution of zooplankton might not be expected to be large, and did not include the contribution of viruses, whose significant contributions were not realized at the time.

Nonetheless, those studies demonstrated dominance of the living biomass in oceanic plankton by the bacterial assemblage (bacteria + archaea), typically followed by contributions of phototrophic picoeukaryotes, coccoid cyanobacteria and then other plankton assemblages. Bacteria have been shown to dominate the total living microbial biomass of the upper water column even in ice-covered regions of the Arctic (Seuthe et al., 2011). The distribution of microbial biomass at the SPOT site is in general agreement with those previous findings. Bacteria contributed very significantly (> 35%) to microbial carbon integrated throughout the top 100 m, with a somewhat larger contribution in the top 500 m (Fig. 5a,b). An increased contribution of bacterial biomass was anticipated in microbial biomass integrated over 500 m, given that bacterial abundances did not decrease as precipitously with depth as was the case for many plankton groups (Figs. 7,8). Indeed, it has been estimated that the deep ocean is the repository for approximately 75% of all prokaryote biomass and a large proportion of all living biomass (Arístegui et al., 2009).

One unique aspect of the present study is our estimate of viral carbon as a component of total microbial biomass. Studies of microbial biomass performed until very recently have ignored the contribution of viral carbon to total living microbial carbon in marine plankton communities. This is, in part, due to the fact that viruses are not technically 'alive', but warrant inclusion because they are capable of commandeering the cellular processes of living cells, and their structures contribute to total organic carbon present in the water column. In the present study, viral abundances exceeded all other microbial assemblages enumerated by > 1–6 orders of magnitude (Table 2), yet viral carbon constituted a rather consistent and modest portion of the total carbon contained in the pelagic community (≈8% of integrated carbon; Figs. 5a,b, 7, 8). This finding is in agreement with present estimates of the global significance of these entities (Suttle, 2005, 2007). Suttle (2007) estimated that marine viruses represent approximately 5% of the total microbial biomass (prokaryotes, viruses, protists). However, significant uncertainties probably remain with the estimation of viral carbon in the ocean. One recent study reported that viral abundances may be overestimated by 13–28% using common counting protocols (Mendes et al., 2014), while conversely, another study has suggested that the contribution of RNA viruses (i.e. eukaryote infective agents) has been substantially underestimated in past studies (Steward et al., 2013). Conversion of viral abundances to carbon biomass is also poorly constrained because the size of individual viruses is highly variable (Jover et al., 2014). We employed a conversion factor in this study that is at the upper end of the range in the literature.

Phototrophic picoplankton (*Synechococcus*, *Prochlorococcus* and phototrophic picoeukaryotes) constituted approximately one quarter of the total depth-integrated microbial carbon in the upper 100 m at the SPOT site (Fig. 5a). Goericke (2011) reported that the contribution of small phytoplankton (picoplankton and small (< 8 μm) nanoplankton within the California Current System) was a large percentage (≈90%) of phytoplankton biomass within the CalCOFI grid. Our results are generally in agreement with those findings (Figs. 7, 8) with the exception that diatoms constituted a larger fraction of total phytoplankton biomass, as might be expected for a more-coastal site such as SPOT. Picoplanktonic phytoplankton at the Bermuda Atlantic Time-series (BATS) station in the Sargasso Sea collectively constituted 1–2 g C m^{-2} in the upper 200 m of the water column (DuRand et al., 2001). The biomass of picoplankton at the SPOT site was similar to the latter estimate (≈1 g C m^{-2} in the upper 100 m; Fig. 5c), even though our coastal site is not as oligotrophic as the BATS site. Phototrophic picoeukaryotes at the SPOT site contributed a somewhat greater fraction of phytoplankton biomass in the euphotic zone than cyanobacteria, especially during spring and summer (Fig. 8).

Nanoplankton biomass (phototrophic/mixotrophic and heterotrophic protists 2–20 μm in size) is a poorly constrained parameter in analyses of plankton biomass, as noted above. Total depth-integrated nanoplankton biomass in this study was a modest component (11–14%) of total microbial biomass (Fig. 5a,b) but slight changes in assumed cell sizes of nanoplankton could easily double that value. Nonetheless, our overall result that nanoplankton contributed a minor fraction of total microbial biomass is in accordance with previous studies that have indicated that nanoplankton biomass is small in comparison to the biomass of picoplankton (Sohrin et al., 2010; Vargas et al., 2012). Heterotrophs exceeded phototrophs in this size category at our study site, perhaps reflecting the near-shore location of the site but also the shallow euphotic zone (Fig. 5a) and therefore limited contribution of phototrophs/mixotrophs to depth-integrated biomass (Table 2; Figs. 5a,b, 7).

The contribution of phagotrophic phytoflagellates (i.e. mixotrophic nanoplankton) to phototrophic nanoplankton in our study is unclear. Published accounts indicate that phagotrophic species can be a significant fraction of the total number of phototrophic nanoplankton in natural plankton communities (Christaki et al., 1999; Unrein et al., 2007; Granda and Anadón, 2008; Moorthi et al., 2009; Vargas et al., 2012), and phagotrophy continues to be demonstrated in an increasing number of phytoplankton species that were formally thought to be exclusively phototrophic (Burkholder et al., 2008; Sanders, 2011; Sanders and Gast, 2011). The contribution of mixotrophs to total microbial biomass at the SPOT site must still have been low, however, because the total contribution of phototrophic nanoplankton (phototrophs + mixotrophs) was typically < 5% of total biomass.

Microplanktonic phytoplankton and zooplankton (20–200 μm) comprised approximately 15% of the total depth-integrated microbial biomass (Fig. 5a) and not more than ≈10 μg C l^{-1} in surface samples at the SPOT sampling site (Figs. 7, 8). Phytoplankton > 20 μm at the site were almost exclusively diatoms and dinoflagellates, with diatoms typically the dominant contributor. Microphytoplankton can occasionally constitute major, but typically highly variable, components of the total phytoplankton biomass in the Southern California Bight due to episodic blooms (Kim et al., 2009; Nezlin et al., 2012; Seubert et al., 2013). The modest contribution of microphytoplankton at our study site indicates the typically oligotrophic nature of this coastal ecosystem just 15 km from the mainland, and is also consistent with the low chlorophyll values observed throughout the year at the SPOT site (Fig. 4). A review of data on diatom biomass globally yielded a median value of ≈11 μg C l^{-1} (Leblanc et al., 2012), a number that is in close agreement with our estimate of diatom biomass at the SPOT site obtained in this study (Figs. 7, 8). Heterotrophic microplankton (ciliate) biomass in our study was always low and never constituted more than a few percent of total microbial biomass (Figs. 5a,b, 7–10).

Our results regarding microbial biomass are very much in agreement with the results of Taylor et al. (2015), who estimated autotrophic

biomass within the CalCOFI study region, including stations within the Channel Islands in the region of the SPOT station. Their southern coastal station closest to the SPOT site yielded estimates of autotrophic carbon that were very consistent with the summed phototroph biomass in the present study (*Synechococcus* + *Prochlorococcus* + photosynthetic picoeukaryotes, nanoplankton and microplankton (note the 5 m and SCM values in Figs. 7, 8)). Such agreement between studies would imply that our choices for conversion factors in the present study were reasonable.

The contribution of mesozooplankton biomass (> 200 μm) averaged < 5% of total plankton biomass throughout the year, with slightly larger contributions during late spring and summer (Fig. 11). Only a few of our highest values (≈5 μg C l^{-1}) were within the range of mesozooplankton biomass values reported for the southern California section of the California Current System, when converted to similar units (Lavaniegos and Ohman, 2007; Décima et al., 2011). Our generally lower values may reflect avoidance of the smaller net used in our study, or inadequate sampling of vertically migrating species (all our tows were conducted during the day). Our estimates of the overall contribution of mesozooplankton biomass relative to that of microbial assemblages, however, fall within the range of more expansive datasets. A global inventory of mesozooplankton biomass in the ocean estimated a value of 0.24 Pg C (Buitenhuis et al., 2010) in that plankton compartment, while bacterial biomass was estimated to be approximately 5× greater at 1.2 Pg C (Buitenhuis et al., 2012). A global analysis of mesozooplankton and macrozooplanton biomass yielded mean values that were comparable (Moriarty et al., 2013; Moriarty and O'Brien, 2013).

Seasonal and monthly estimates of depth-specific and depth-integrated biomass values (Figs. 8–10) for the various plankton groups revealed modest levels of variability on those times scales. Depth-specific biomass estimates during spring and summer were ≈40% greater than values during fall and winter (Fig. 8). Month-to-month variability in depth-integrated biomass (Fig. 9c,d) was somewhat greater than seasonal variability (Fig. 10c,d), except for a few months when microbial biomass was approximately double most other months. Relatively low seasonal variability reflects the subtropical nature of the SPOT site with its small annual amplitudes of temperature and other chemical/physical parameters (Fig. 2). The monthly and seasonal variability in standing stocks of microbial biomass is consistent with previously reported values of monthly-to-interannual variability observed at the sampling site, and even small-scale temporal and spatial variability (Chow et al., 2013; Kim et al., 2013; Lie et al., 2013).

The concentrations of total heterotrophic microbial biomass and total phototrophic microbial biomass were relatively equitable at the SPOT site (Figs. 5a,b, 7). The significant proportion of heterotrophs was largely a consequence of the large contribution of bacterial biomass. Roman et al. (1995) noted that carbon among the heterotrophic assemblages in surface waters of the Sargasso Sea was greater than carbon contained in phototrophs during the summer, but was more equitable in spring. The authors noted that the partitioning of living biomass in the upper 100 m was not a broad-based pyramid with photosynthetic biomass exceeding heterotrophic biomass. The situation appears to be similar at our coastal site. Our results indicate that heterotrophic microbial carbon at our study site constituted approximately 2 g C m^{-2} integrated throughout the top 100 m (Fig. 5c). Sohrin et al. (2010) reviewed depth-integrated carbon biomass values for heterotrophic prokaryotes, heterotrophic nanoflagellates and ciliates from various epipelagic oceanic ecosystems (see their Table 6). Values generally ranged from a few 10 s mg C m^{-2} to > 2 g C m^{-2} in the upper 100 m, values in agreement with our findings.

4.3. Contribution of microbial biomass to POC and flux

To our knowledge, our study is the most complete assessment of the microbial assemblages of a planktonic community to date. Numerous studies have investigated specific components of planktonic communities (e.g. phytoplankton, bacteria or viruses) but complete assessments are rare because of the various expertise and methodologies required to characterize all microbial groups. In particular, most studies that have counted viruses have not placed these entities into a community framework. Our study therefore enables an assessment of the relative contributions of specific plankton groups to total microbial organic carbon and total microbial biomass to POC at our study site in the eastern North Pacific.

Our estimates of microbial biomass in the upper water column (≈60 μg C l^{-1}; Fig. 7) and depth-integrated microbial carbon within the upper 100 m (≈4 g C m^{-2}; Fig. 5c) fall within the range of values estimated in other oceanic provinces (Ishizaka et al., 1997; Garrison et al., 2000), regionally in the Southern California Current Ecosystem (Taylor et al., 2015), and one previous study in the San Pedro Basin (Nelson et al., 1987). Global databases of POC in surface waters occur over a wide range in the world ocean from < 10 to > 1000 μg C l^{-1} (< 1 to > 100 μM C) across ecosystems spanning oligotrophic oceanic gyres to highly productive coastal environments (Gardner et al., 2006; Stramski et al., 2008). The amount of living microbial biomass is generally considered to be a significant component of the total POC, even in highly oligotrophic ecosystems (Roman et al., 1995; Kawasaki et al., 2011). POC was not routinely measured as a part of the San Pedro Ocean Time-series during our study, but typical standing stocks of POC in the Santa Barbara basin to the north of the San Pedro Basin have been reported to range between ≈500 and 3700 μg C l^{-1} (Shipe et al., 2002). This range of values implies that microbial carbon at the SPOT site constitutes only a few to > 10% of total POC in surface waters, although the waters of the Santa Barbara basin are more productive than the San Pedro Basin and thus may be a poor indicator of total POC at the SPOT site. Martiny (2016) noted that microbial carbon constituted > 40% (median) of the POC in samples collected at a pier located at Newport Beach, CA, approximately 30 km to the east of our sampling site. Studies in the Sargasso Sea and Arabian Sea have reported that the carbon content of the microbial community in those regions comprised approximately 25–50% of total POC (Caron et al., 1995; Garrison et al., 2000). Our low values may indicate that the conversion factors employed in the present study were overly conservative for estimating microbial biomass.

Standing stocks of microbial assemblages in surface waters of the San Pedro Basin place constraints on their potential contribution to water column processes as well as their contribution to the sinking of POC into deep water in the basin. Simple mass balance calculations provide confirmation that the values we obtained in the present study are realistic in relation to flux measurements. For example, the vertical flux of organic carbon out of the euphotic zone in the Santa Monica and San Pedro Basins has been estimated to range seasonally from ≈20 to > 150 mg C $m^{-2}d^{-1}$ (Nelson et al., 1987; Thunell et al., 1994; Berelson and Stott, 2003; Collins et al., 2011; Haskell, 2015; Haskell et al., 2016). Estimated phytoplankton biomass in surface waters at the SPOT site in the present study averaged 22 μg C l^{-1} in samples within the euphotic zone (Fig. 7). This value corresponds to an integrated phytoplankton biomass of 880 mg C m^{-2}, assuming a 40 m euphotic zone (Fig. 3). Given that value for the phytoplankton standing stock, and assuming a rate of primary production equivalent to a doubling time of two days for the phytoplankton assemblage, a vertical flux of ≈10% of primary production could support a vertical flux of 44 mg C m^{-2} d^{-1}. There is, therefore, good agreement between values obtained from these disparate studies and measurements.

An interesting observation in our study was the high relative abundances of diatoms in samples collected at 150 and 500 m (Figs. 7, 8). This unexpected result may in part be a consequence of including non-living diatoms with frustules containing cellular debris as living cells. However, it has been noted that the vertical flux of matter into sediment traps at 550 m and 800 m in the San Pedro Basin was strongly and closely correlated (Collins et al., 2011), while other

studies in the region have implicated rapid transport of material into deeper waters during periods of high flux (Sekula-Wood et al., 2009; Bishop et al., 2016). Nelson et al. (1987) noted that intact phytoplankton were a minor but measurable component of sediment trap material, and generally larger contributions were episodic and coincided with phytoplankton blooms in the region. Our observation that diatoms contributed significantly to total microbial biomass in deeper samples in San Pedro Basin (Fig. 7) may imply a significant and relatively constant contribution of diatoms to sinking particles at the SPOT site.

4.4. Concluding remarks

A predictive understanding of biogeochemical processes in coastal pelagic ecosystems, and how they might respond to environmental change (either natural or anthropogenic), is predicated on knowledge of the microbial taxa that dominate those ecosystems. This study provides the most complete assessment to date of the organic carbon associated with the various microbial assemblages of a coastal planktonic community, as well as the vertical, monthly and seasonal variability associated with these assemblages, at the site of a long-term microbial oceanographic time series. Studies during the past few decades have provided great insight into the species diversity and activities of microbial communities, made possible largely through the application of cutting-edge genetic approaches (DeLong and Karl, 2005; Caron, 2009). Characterizing the biomass associated with this vast array of microbes has garnered less attention in recent years but is also essential for helping constrain the potential activities of these assemblages in natural aquatic communities. Coupled to diversity and rate measurements conducted, the analysis contained in this study enables in-depth analysis and modeling of microbial processes and carbon and energy flow in the coastal ecosystem off Southern California (Landry et al., 2009; Connell et al., In preparation).

Acknowledgements

This work was supported by National Science Foundation grants MCB-0703159, MCB-0084231 and OCE-1136818. The authors thank the Captain and Crew of the R/V Yellowfin, Troy Gunderson for CTD operations and processing of environmental samples, the Wrigley Institute for Environmental Studies for fieldwork support, and an anonymous reviewer who offered comments that were helpful for improving the discussion of microbial biomass estimation.

References

Aksnes, D.L., Ohman, M.D., 2009. Multi-decadal shoaling of the euphotic zone in the southern sector of the California Current System. Ecol. Res. 54, 1272–1281.
Alber, M., Reed, D., McGlathery, K., 2013. Coastal long term ecological research: introduction to the special issue. Oceanography 26, 14–17.
Anderson, T.R., Ducklow, H.W., 2001. Microbial loop carbon cycling in ocean environments studied using a simple steady-state model. Aq. Microb. Ecol. 26, 37–49.
Arístegui, J., Gasol, J.M., Duarte, C.M., Herndl, G.J., 2009. Microbial oceanography of the dark ocean's pelagic realm. Limnol. Oceanogr. 54, 1501–1529.
Beman, J.M., Steele, J., Fuhrman, J.A., 2011. Co-occurrence patterns for abundant marine archaeal and bacterial lingeages in the deep chlorophyll maximum of coastal California. ISME J..
Berelson, W.M., 1991. The flushing of two deep-sea basins, southern California borderland. Limnol. Oceanogr 36, 1150–1166.
Berelson, W.M., Stott, L.D., 2003. Productivity and organic carbon rain to the California margin seafloor: modern and paleoceanographic perspectives. Paleoceanography 18, 1002.
Bishop, J.K.B., Fong, M.B., Wood, T.J., 2016. Robotic observations of high wintertime carbon export in California coastal waters. Biogeosci. Discuss. 2016, 1–32.
Bode, A., Álvarez-Ossorio, M.T., González, N., 1998. Estimations of mesozooplankton biomass in a coastal upwelling area off NW Spain. J. Plankton Res. 20, 1005–1014.
Brown, S.L., Landry, M.R., Neveux, J., Dupouy, C., 2003. Microbial community abundance and biomass along a 180 degrees transect in the equatorial Pacific during an El Nino-Southern Oscillation cold phase. J. Geophys. Res. (Oceans) 108.
Buck, K.R., Chavez, F.P., Campbell, L., 1996. Basin-wide distributions of living carbon components and the inverted trophic pyramid of the central gyre of the North Atlantic Ocean, summer 1993. Aquat. Microb. Ecol. 10, 283–298.
Buitenhuis, E.T., Li, W.K.W., Lomas, M.W., Karl, D.M., Landry, M.R., Jacquet, S., 2012. Bacterial biomass distribution in the global ocean. Earth Syst. Sci. Data Discuss. 5, 301–315.
Buitenhuis, E.T., Rivkin, R.B., Sailley, S., Le Quéré, C., 2010. Biogeochemical fluxes through microzooplankton. Glob. Biogeochem., (Cycles 24, GB4015).
Burkholder, J.M., Glibert, P.M., Skelton, H.M., 2008. Mixotrophy, a major mode of nutrition for harmful algal species in eutrophic waters. Harmful Algae 8, 77–93.
Calbet, A., Landry, M.R., 2004. Phytoplankton growth, microzooplankton grazing, and carbon cycling in marine systems. Limnol. Oceanogr. 49, 51–57.
Calbet, A., Saiz, E., 2005. The ciliate-copepod link in marine food ecosystems. Aq. Microb. Ecol. 38, 157–167.
Caron, D.A., 2009. New accomplishments and approaches for assessing protistan diversity and ecology in natural ecosystems. BioScience 59, 287–299.
Caron, D.A., Countway, P.D., Jones, A.C., Kim, D.Y., Schnetzer, A., 2012. Marine protistan diversity. Ann. Rev. Mar. Sci. 4, 467–493.
Caron, D.A., Dam, H.G., Kremer, P., Lessard, E.J., Madin, L.P., Malone, T.C., Napp, J.M., Peele, E.R., Roman, M.R., Youngbluth, M.J., 1995. The contribution of microorganisms to particulate carbon and nitrogen in surface waters of the Sargasso Sea near Bermuda. Deep-Sea Res. 42, 943–972.
Casey, J.R., Aucan, J.P., Goldberg, S.R., Lomas, M.W., 2013. Changes in partitioning of carbon amongst photosynthetic pico- and nano-plankton groups in the Sargasso Sea in response to changes in the North Atlantic Oscillation. Deep-Sea Res. II 93, 58–70.
Cheung, W.W.L., Watson, R., Pauly, D., 2013. Signature of ocean warming in global fisheries catch. Nature 497, 365–368.
Cho, B.C., Azam, F., 1990. Biogeochemical significance of bacterial biomass in the ocean's euphotic zone. Mar. Ecol. Prog. Ser. 63, 253–259.
Chow, C.-E.T., Fuhrman, J.A., 2012. Seasonality and monthly dynamics of marine myovirus communities. Environ. Microbiol. 14, 2171–2183.
Chow, C.-E.T., Kim, D.Y., Sachdeva, R., Caron, D.A., Fuhrman, J.A., 2014. Top-down controls on bacterial community structure: microbial network analysis of bacteria, T4-like viruses and protists. ISME J. 8, 816–829.
Chow, C.-E.T., Sachdeva, R., Cram, J.A., Steele, J.A., Needham, D.M., Patel, A., Parada, A.E., Fuhrman, J.A., 2013. Temporal variability and coherence of euphotic zone bacterial communities over a decade in the Southern California Bight. ISME J. 7, 2259–2273.
Christaki, U., Van Wambeke, F., Dolan, J.R., 1999. Nanoflagellates (mixotrophs, heterotrophs and autotrophs) in the oligotrophic eastern Mediterranean: standing stocks, bacterivory and relationships with bacterial production. Mar. Ecol. Prog. Ser. 181, 297–307.
Church, M.J., Wai, B., Karl, D.M., DeLong, E.F., 2010. Abundances of crenarchaeal amoA genes and transcripts in the Pacific Ocean. Environ. Microbiol. 12, 679–688.
Collins, L.E., Berelson, W., Hammond, D.E., Knapp, A., Schwartz, R., Capone, D., 2011. Particle fluxes in San Pedro Basin, California: a four-year record of sedimentation and physical forcing. Deep-Sea Res. I 58, 898–914.
Connell, P.E., Campbell, V., Gellene, A.G., Hu, S.K., Caron, D.A., 2017. Planktonic food web structure at a coastal time-series site: II. Spatiotemporal variability of microbial trophic activities. Deep Sea Res., in preparation
Countway, P.D., Vigil, P.D., Schnetzer, A., Moorthi, S.D., Caron, D.A., 2010. Seasonal analysis of protistan community structure and diversity at the USC Microbial Observatory (San Pedro Channel, North Pacific Ocean). Limnol. Oceanogr. 55, 2381–2396.
Cram, J.A., Chow, C.-E.T., Sachdeva, R., Needham, D.M., Parada, A.E., Steele, J.A., Fuhrman, J.A., 2014. Seasonal and interannual variability of the marine bacterioplankton community throughout the water column over ten years. ISME J..
Décima, M., Landry, M.R., Rykaczewski, R.R., 2011. Broad scale patterns in mesozooplankton biomass and grazing in the eastern equatorial Pacific. Deep-Sea Res. II 58, 387–399.
del Giorgio, P.A., Bird, D.F., Prairie, Y.T., Planas, D., 1996. Flow cytometric determination of bacterial abundance in lake plankton with the green nucleic acid stain SYTO 13. Appl. Environ. Microbiol. 41, 783–789.
DeLong, E.F., Karl, D.M., 2005. Genomic perspectives in microbial oceanography. Nature 437, 336–342.
Dennett, M.R., Mathot, S., Caron, D.A., Smith, W.O., Lonsdale, D.J., 2001. Abundance and distribution of phototrophic and heterotrophic nano- and microplankton in the southern Ross Sea. Deep-Sea Res. II 48, 4019–4037.
Duarte, C.M., Regaudie-de-Gioux, A., Arrieta, J.M., Delgado-Huertas, A., Agustí, S., 2013. The Oligotrophic Ocean Is Heterotrophic*. Ann. Rev. Mar. Sci. 5, 551–569.
Ducklow, H.W., Doney, S.C., 2013. What is the metabolic state of the oligotrophic ocean? A Debate. Ann. Rev. Mar. Sci. 5, 525–533.
DuRand, M.D., Olson, R.J., Chisholm, S.W., 2001. Phytoplankton population dynamics at the Bermuda Atlantic Time-series station in the Sargasso Sea. Deep-Sea Res. II 48, 1983–2003.
Fuhrman, J.A., 2009. Microbial community structure and its functional implications. Nature 459, 193–199.
Fuhrman, J.A., Steele, J., Sun, F., Xia, L., Countway, P.D., Caron, D.A. American Society of Limnology and Oceangraphy, Nice, France, 2009.
Fukuda, R., Ogawa, H., Nagata, T., Koike, I., 1998. Direct determination of carbon and nitrogen contents of natural bacterial assemblages in marine environments. Appl. Environ. Microbiol. 64, 3352–3358.
Gardner, W.D., Mishonov, A.V., Richardson, M.J., 2006. Global POC concentrations from in-situ and satellite data. Deep-Sea Res. II 53, 718–740.
Garrison, D.L., Gowing, M.M., Hughes, M.P., Campbell, L., Caron, D.A., Dennett, M.R., Shalapyonok, A., Olson, R.J., Landry, M.R., Brown, S.L., Liu, H.B., Azam, F., Steward, G.F., Ducklow, H.W., Smith, D.C., 2000. Microbial food web structure in the Arabian Sea: a US JGOFS study. Deep-Sea Res. II 47, 1387–1422.
Goericke, R., 2011. The size structure of marine phytoplankton - what are the rules?

CalCOFI Rep. 52, 198–204.
Gordon, L.I., Jennings, J.J.C., Ross, A.A., Krest, J.M., 1993. A suggested protocol for continuous flow automated analysis of seawater nutrients (phosphate, nitrate, nitrite and silicic acid) in the WOCE Hydrographic Program and the Joint Global Ocean Fluxes Study, WHP Operations And Methods. College of Oceanic and Atmospheric Sciences Oregon State University, Corvallis, Oregon.
Granda, A.P., Anadón, R., 2008. The annual cycle of nanoflagellates in the central Cantabrian Sea (Bay of Biscay). J. Mar. Syst. 72, 298–308.
Grasshoff, K., Kremling, K., Ehrhardt, M., 2007. Methods of Seawater Anlaysis. Wiley-VCH GmbH, Weinheim, Germany.
Hales, B., Takahashi, T., Bandstra, L., 2005. Atmospheric CO_2 uptake by a coastal upwelling system. Glob. Biogeochem., (Cycles 19, GB1009).
Hamersley, M.R., Turk, K.A., Leinweber, A., Gruber, N., Zehr, J.P., Gunderson, T., Capone, D.G., 2011. Nitrogen fixation within the water column associated with two hypoxic basins in the Southern California Bight. Aq. Microb. Ecol. 63, 193–205.
Harris, R.P., Wiebe, P.H., Lenz, J., Skjoldal, H.R., Huntley, M., 2000. Zooplankton Methodology Manual. Academic Press, London, 684.
Haskell, W.Z., II, 2015. Ecosystem Export Efficiency in an Upwelling Region: A Two-year Time Series Study of Vertical Transport, Particle Export and In-situ Net and Gorss Oxygen Production (Ph.D. thesis). University of Southern California, Los Angeles, 305.
Haskell, W.Z., II, Prokopenko, M.G., Hammond, D.E., Stanley, R.H.R., Berelson, W., Baronas, J.J., Fleming, J.C., Aluwihare, L., 2016. An organic carbon budget for coastal Southern California determined by estimates of vertical nutrient flux, net community production and export. Deep-Sea Res. 116, 49–75.
Hofmann, G.E., Blanchette, C.A., Rivest, E.B., Kapsenberg, L., 2013. Taking the pulse of marine ecosystems: the importance of coupling long-term physical and biological observations in the context of global change biology. Oceanography 26, 140–148.
Hood, R.R., Laws, E.A., Armstrong, R.A., Bates, N.R., Brown, C.W., Carlson, C.A., Chai, F., Doney, S.C., Falkowski, P.G., Feely, R.A., Friedrichs, M.A.M., Landry, M.R., Keith Moore, J., Nelson, D.M., Richardson, T.L., Salihoglu, B., Schartau, M., Toole, D.A., Wiggert, J.D., 2006. Pelagic functional group modeling: progress, challenges and prospects. Deep-Sea Res. II 53, 459–512.
Howard, M.D.A., Sutula, M., Caron, D.A., Chao, Y., Farrara, J.D., Frenzel, H., Jones, B., Robertson, G., McLaughlin, K., Sengupta, A., 2014. Anthropogenic nutrient sources rival natural sources on small scales in the coastal waters of the Southern California Bight. Limnol. Oceanogr. 59, 285–297.
Ishizaka, J., Harada, K., Ishikawa, K., Kiyosawa, H., Furusawa, H., Watanabe, Y., Ishida, H., Suzuki, K., Handa, N., Takahashi, M., 1997. Size and taxonomic plankton community structure and carbon flow at the equator, 175°E during 1990–1994. Deep-Sea Res. II 44, 1927–1949.
Jover, L.F., Effler, T.C., Buchan, A., Wilhelm, S.W., Weitz, J.S., 2014. The elemental composition of virus particles: implications for marine biogeochemical cycles. Nat. Rev. Microbiol. 12, 519–528.
Kahru, M., Kudela, R., Manzano-Sarabia, M., Mitchell, B.G., 2009. Trends in primary production in the California Current detected with satellite data. J. Geophys. Res.: Oceans 114, C02004.
Karl, D.M., Church, M.J., 2014. Microbial oceanography and the Hawaii Ocean Time-series programme. Nat. Rev. Microbiol 12, 699–713.
Karl, D.M., Michaels, A.F., 1996. The Hawaiian Ocean Time-series (HOT) and Bermuda Atlantic Time-series study (BATS). . Deep-Sea Res. II 43, 127–128.
Kawasaki, N., Sohrin, R., Ogawa, H., Nagata, T., Benner, R., 2011. Bacterial carbon content and the living and detrital bacterial contributions to suspended particulate organic carbon in the North Pacific Ocean. Aq. Microb. Ecol. 62, 165–176.
Kepner, R.L., Wharton, R.A., Suttle, C.A., 1998. Viruses in Antarctic lakes. Limnol. Oceanogr. 43, 1754–1761.
Kim, D.Y., Countway, P.D., Jones, A.C., Schnetzer, A., Yamashita, W., Tung, C., Caron, D.A., 2013. Monthly to interannual variability of microbial eukaryote assemblages at four depths in the eastern North Pacific. ISME J..
Kim, H.-J., Miller, A.J., McGowan, J., Carter, M.L., 2009. Coastal phytoplankton blooms in the Southern California Bight. Prog. Oceanogr. 82, 137–147.
Kudela, R.M., Pitcher, G., Probyn, T., Figueiras, F., Moita, T., Trainer, V.L., 2005. Harmful algae blooms in coastal upwelling systems. Oceanography 18, 184–197.
Landry, M.R., Ohman, M.D., Goericke, R., Stukel, M.R., Tsyrklevich, K., 2009. Lagrangian studies of phytoplankton growth and grazing relationships in a coastal upwelling ecosystem off Southern California. Prog. Oceanogr. 83, 208–216.
Lavaniegos, B.E., Ohman, M.D., 2007. Coherence of long-term variations of zooplankton in two sectors of the California Current System. Prog. Oceanogr. 75, 42–69.
Leblanc, K., Arístegui, J., Armand, L., Assmy, P., Beker, B., Bode, A., Breton, E., Cornet, V., Gibson, J., Gosselin, M.-P., Kopczynska, E., Marshall, H., Peloquin, J., Piontkovski, S., Poulton, A.J., Quéguiner, B., Schiebel, R., Shipe, R., Stefels, J., van Leeuwe, M.A., Varela, M., Widdicombe, C., Yallop, M., 2012. A global diatom database - abundance, biovolume and biomass in the world ocean. Earth Syst. Sci. Data 4, 149–165.
Lee, S., Fuhrman, J.A., 1987. Relationships between biovolume and biomass of naturally derived marine bacterioplankton. Appl. Environ. Microbiol. 53, 1298–1303.
Levitus, S., 1982. Climatological atlas of the world ocean, Rockville, MD
Li, W.K.W., Dickie, P.M., Irwin, B.D., Wood, A.M., 1992. Biomass of bacteria, cyanobacteria, prochlorophytes and photosynthetic eukaryotes in the Sargasso Sea. Deep-Sea Res. 39, 501–519.
Lie, A.A.Y., Kim, D.Y., Schnetzer, A., Caron, D.A., 2013. Small-scale temporal and spatial variations in protistan community composition at the San Pedro Ocean Time-series station off the coast of southern California. Aquat. Microb. Ecol. 70, 93–110.
Martiny, A.C., Talarmin, A., Mouginot, C., Lee, J.A., Huang, J.S., Gellene, A.G., Caron, D.A., 2016. Biogeochemical interactions control a temporal succession in the elemental composition of marine communities. Limnol. Oceanogr. 61, 531–542.
McMahon, K.W., McCarthy, M.D., Sherwood, O.A., Larsen, T., Guilderson, T.P., 2015. Millennial-scale plankton regime shifts in the subtropical North Pacific Ocean. Science 350, 1530–1533.
Menden-Deuer, S., Lessard, E.J., 2000. Carbon to volume relationships for dinoflagellates, diatoms, and other protist plankton. Limnol. Oceanogr. 45, 569–579.
Mendes, C., Santos, Ls, Cunha, Ç., Gomez, N.M., Almeida, A., 2014. Proportion of prokaryotes enumerated as viruses by epifluorescence microscopy. Ann. Microbiol. 64, 773–778.
Moorthi, S.D., Caron, D.A., Gast, R.J., Sanders, R.W., 2009. Mixotrophy: a widespread and important ecological strategy for planktonic and sea-ice nanoflagellates in the Ross Sea, Antarctica. Aquat. Microb. Ecol. 54, 269–277.
Moriarty, R., Buitenhuis, E.T., Le Quére, C., Gosselin, M.-P., 2013. Distribution of known macrozooplankton abundance and biomass in the global ocean. Earth Syst. Sci. Data 5, 241–257.
Moriarty, R., O'Brien, T.D., 2013. Distribution of mesozooplankton biomass in the global ocean. Earth Syst. Sci. Data 5, 45–55.
Nelson, J.R., Beers, J.R., Eppley, R.W., Jackson, G.A., McCarthy, J.J., Soutar, A., 1987. A particle flux study in the Santa Monica-San Pedro Basin off Los Angeles: particle flux, primary production, and transmissometer survey. Cont. Shelf Res. 7, 307–328.
Nezlin, N.P., Sutula, M.A., Stumpf, R.P., Sengupta, A., 2012. Phytoplankton blooms detected by SeaWiFS along the central and southern California coast. J. Geophys. Res. -Oceans, 117. http://dx.doi.org/10.1029/2011jc007773.
Noble, R.T., Fuhrman, J.A., 1998. Use of SYBR Green I for rapid epifluorescence counts of marine viruses and bacteria. Aquat. Microb. Ecol. 14, 113–118.
Parsons, T.R., Maita, Y., Lalli, C.M., 1984. A Manual of Chemical and Biological Methods for Seawater Analysis. Pergamon Press, Oxford, 173.
Roman, M.R., Caron, D.A., Kremer, P., Lessard, E.J., Madin, L.P., Malone, T.C., Napp, J.M., Peele, E.R., Youngbluth, M.J., 1995. Spatial and temporal changes in the partitioning of organic carbon in the plankton community of the Sargasso Sea off Bermuda. Deep-Sea Res. I 42, 973–992.
Rykaczewski, R.R., Dunne, J.P., 2010. Enhanced nutrient supply to the California Current Ecosystem with global warming and increased stratification in an earth system model. Geophys. Res. Lett. 37, L21606.
Samuelsson, K., Berglund, J., Haecky, P., Andersson, A., 2002. Structural changes in an aquatic microbial food web caused by inorganic nutrient addition. Aquat. Microb. Ecol. 29, 29–38.
Sanders, R.W., 2011. Alternative nutritional strategies in protists: symposium introduction and a review of freshwater protists that combine photosynthesis and heterotrophy1. J. Eukary. Microbiol. 58, 181–184.
Sanders, R.W., Gast, R.J., 2011. Bacterivory by phototrophic picoplankton and nanoplankton in Arctic waters. FEMS Microbiol. Ecol. 82, 242–253.
Sanders, R.W., Porter, K.G., 1988. Phagotrophic phytoflagellates. Adv. Microb. Ecol. 10, 167–192.
Schnetzer, A., Miller, P.E., Schnaffner, R.A., Stauffer, B.A., Jones, B.H., Weisberg, S.B., DiGiacomo, P.M., Berelson, W.M., Caron, D.A., 2007. Blooms of Pseudo-nitzschia and domoic acid in the San Pedro Channel and Los Angeles harbor areas of the Southern California Bight, 2003–2004. Harmful Algae 6, 372–387.
Schnetzer, A., Moorthi, S.D., Countway, P.D., Gast, R.J., Gilg, I.C., Caron, D.A., 2011. Depth matters: microbial eukaryote diversity and community structure in the eastern North Pacific revealed through environmental gene libraries. Deep-Sea Res. I 58, 16–26.
Sekula-Wood, E., Schnetzer, A., Benitez-Nelson, C.R., Anderson, C., Berelson, W., Brzezinksi, M., Burns, J., Caron, D.A., Cetinic, I., Ferry, J., Fitzpatrick, E., Jones, B., Miller, P.E., Morton, S.L., Schaffner, R., Siegel, D., Thunell, R., 2009. Rapid downward transport of the neurotoxin domoic acid in coastal waters. Nat. Geosci. 2, 272–275.
Seubert, E.L., Gellene, A.G., Howard, M.D.A., Connell, P., Ragan, M., Jones, B.H., Runyan, J., Caron, D.A., 2013. Seasonal and annual dynamics of harmful algae and algal toxins revealed through weekly monitoring at two coastal ocean sites off southern California, USA. Environ. Sci. Pollut. Res. 20, 6878–6895.
Seuthe, L., Töpper, B., Reigstad, M., Thyrhaug, R., Vaquer-Sunyer, R., 2011. Microbial communities and processes in ice-covered Arctic waters of the northwestern Fram Strait (75 to 80°N) during the vernal pre-bloom phase. Aquat. Microb. Ecol. 64, 253–266.
Sherr, B.F., Sherr, E.B., Caron, D.A., Vaulot, D., Worden, A.Z., 2007. A sea of microbes: oceanic protists. Oceanography 20, 102–106.
Sherr, E.B., Caron, D.A., Sherr, B.F., 1993. Staining of heterotrophic protists for visualization via epifluorescence microscopy. In: Kemp, P., Sherr, B., Sherr, E., Cole, J. (Eds.), Handbook of Methods in Aquatic Microbial Ecology. Lewis Publishers, Boca Raton, 213–227.
Sherr, E.B., Sherr, B.F., 2007. Heterotrophic dinoflagellates: a signficant component of microzooplankton biomass and major grazers of diatoms in the sea. Mar. Ecol. Prog. Ser. 352, 187–197.
Shipe, R.F., Passow, U., Brzezinski, M.A., Graham, W.M., Pak, D.K., Siegel, D.A., Alldredge, A.L., 2002. Effects of the 1997-98 El Niño on seasonal variations in suspended and sinking particles in the Santa Barbara basin. Prog. Oceanogr. 54, 105–127.
Sohrin, R., Imazawa, M., Fukuda, H., Suzuki, Y., 2010. Full-depth profiles of prokaryotes, heterotrophic nanoflagellates, and ciliates along a transect from the equatorial to the subarctic central Pacific Ocean. Deep-Sea Res. II 57, 1537–1550.
Steele, J.A., Countway, P.D., Xia, L., Vigil, P.D., Beman, J.M., Kim, D.Y., Chow, C.-E.T., Sachdeva, R., Jones, A.C., Schwalbach, M.S., Rose, J.M., Hewson, I., Patel, A., Sun, F., Caron, D.A., Fuhrman, J.A., 2011. Marine bacterial, archaeal and protistan association networks reveal ecological linkages. ISME J. 5, 1414–1425.
Steinberg, D.K., Carlson, C.A., Bates, N.R., Johnson, R.J., Michaels, A.F., Knap, A.H., 2001. Overview of the US JGOFS Bermuda Atlantic Time-series Study (BATS): a

decade-scale look at ocean biology and biogeochemistry. Deep-Sea Res. II 48, 1405–1447.
Steward, G.F., Culley, A.I., Mueller, J.A., Wood-Charlson, E.M., Belcaid, M., Poisson, G., 2013. Are we missing half of the viruses in the ocean[quest]. ISME J. 7, 672–679.
Stoecker, R.K., Gustafson, D.E., Verity, P.G., 1996. Micro- and mesoprotozooplankton at 140°W in the equatorial Pacific: heterotrophs and mixotrophs. Aquat. Microb. Ecol. 10, 273–282.
Stramski, D., Reynolds, R.A., Babin, M., Kaczmarek, S., Lewis, M.R., Röttgers, R., Sciandra, A., Stramska, M., Twardowski, M.S., Franz, B.A., Claustre, H., 2008. Relationships between the surface concentration of particulate organic carbon and optical properties in the eastern South Pacific and eastern Atlantic Oceans. Biogeosciences 5, 171–201.
Suttle, C.A., 2005. Viruses in the sea. Nature 437, 356–361.
Suttle, C.A., 2007. Marine viruses - major players in the global ecosystem. Nat. Rev. Microbiol. 5, 801–812.
Sydeman, W.J., García-Reyes, M., Schoeman, D.S., Rykaczewski, R.R., Thompson, S.A., Black, B.A., Bograd, S.J., 2014. Climate change and wind intensification in coastal upwelling ecosystems. Science 345, 77–80.
Taylor, A.G., Landry, M.R., Selph, K.E., Wokuluk, J.J., 2015. Temporal and spatial patterns of microbial community biomass and composition in the Southern California Current Ecosystem. Deep-Sea Res. II 112, 117–128.
Thunell, R.C., Pilskaln, C.H., Tappa, E., Sautter, L.R., 1994. Temporal variability in sediment fluxes in the San Pedro Basin, southern California bight. Cont. Shelf Res. 14, 333–352.
Unrein, F., Massana, R., Alonso-Sáez, L., Gasol, J.M., 2007. Significant year-round effect of small mixotrophic flagellates on bacterioplankton in an oligotrophic coastal system. Limnol. Oceanogr. 52, 456–469.
Utermöhl, H., 1958. Zur Vervollkommung der quantitativen phytoplankton-methodik. Mitt. Int. Ver. Limnol. 9, 38.
Vargas, C., Contreras, P., Iriarte, J., 2012. Relative importance of phototrophic, heterotrophic, and mixotrophic nanoflagellates in the microbial food web of a river-influenced coastal upwelling area. Aquat. Microb. Ecol. 65, 233–248.
Veldhuis, M.J.W., Kraay, G.W., van Bleijswijk, J.D.L., Baars, M.A., 1997. Seasonal and spatial variability in phytoplankton biomass, productivity and growth in the norhtwestern Indian Ocean: the southwest and northeast monsoon, 1992–1993. Deep-Sea Res. 44, 425–449.
Wiebe, P.H., Boyd, S., Cox, J.L., 1975. Relationships between zooplankton displacement volume, wet weight, dry weight,and carbon. Fish. Bull. 73, 777–786.
Williams, P.Jl.B., Quay, P.D., Westberry, T.K., Behrenfeld, M.J., 2013. The oligotrophic ocean is autotrophic. Ann. Rev. Mar. Sci. 5, 535–549.
Worden, A.Z., Nolan, J.K., Palenik, B., 2004. Assessing the dynamics and ecology of marine picophytoplankton: the importance of the eukaryotic component. Limnol. Oceanogr. 49, 168–179.